Department of
Industry and Resources

RECORD
2003/15

STRUCTURE AND TECTONICS OF THE LEEUWIN COMPLEX AND DARLING FAULT ZONE, SOUTHERN PINJARRA OROGEN WESTERN AUSTRALIA — A FIELD GUIDE

by D. P. Janssen, A. S. Collins,
and I. C. W. Fitzsimons

SGTSG
Kalbarri
2003

GEOLOGICAL SOCIETY OF AUSTRALIA SPECIALIST GROUP IN TECTONICS AND STRUCTURAL GEOLOGY 12TH FIELD CONFERENCE

Geological Survey of Western Australia

Geological Society of Australia
Specialist Group in Tectonics and Structural Geology
12th Field Conference
Kalbarri, Western Australia, 2003

Sponsored by

GEOLOGICAL SURVEY OF WESTERN AUSTRALIA

Record 2003/15

STRUCTURE AND TECTONICS OF THE LEEUWIN COMPLEX AND DARLING FAULT ZONE, SOUTHERN PINJARRA OROGEN, WESTERN AUSTRALIA — A FIELD GUIDE

by
D. P. Janssen[1], A. S. Collins[1], and I. C. W. Fitzsimons[1]

[1] Tectonics Special Research Centre, Department of Applied Geology, Curtin University of Technology, PO Box U 1987, W.A. 6845

Geological Society of Australia
Specialist Group in Tectonics and Structural Geology
Field Guide No. 12

Perth 2003

MINISTER FOR STATE DEVELOPMENT
Hon. Clive Brown MLA

DIRECTOR GENERAL, DEPARTMENT OF INDUSTRY AND RESOURCES
Jim Limerick

DIRECTOR, GEOLOGICAL SURVEY OF WESTERN AUSTRALIA
Tim Griffin

Notice to users of this guide:
This field guide was published by the Geological Survey of Western Australia (GSWA) for excursions conducted by the Specialist Group in Tectonics and Structural Geology (of the Geological Society of Australia) field conference held in Kalbarri, Western Australia, in September 2003. Authorship of these guides included contributors from the Tectonics Special Research Centres of Curtin University of Technology and University of Western Australia, and GSWA. Editing of the manuscript was restricted to bringing them into GSWA house style. The scientific content of each guide was the responsibility of the authors.

REFERENCE
The recommended reference for this publication is:
JANSSEN, D. P., COLLINS, A. S., and FITZSIMONS, I. C. W., 2003, Structure and tectonics of the Leeuwin Complex and Darling Fault Zone, southern Pinjarra Orogen, Western Australia — a field guide: Western Australia Geological Survey, Record 2003/15, 33p.

National Library of Australia Card Number and ISBN 0 7307 8935 7

Published 2003 by Geological Survey of Western Australia

Copies available from:
Information Centre
Department of Industry and Resources
100 Plain Street
EAST PERTH, WESTERN AUSTRALIA 6004
Telephone: (08) 9222 3459 Facsimile: (08) 9222 3444
This and other publications of the Geological Survey of Western Australia may be viewed or purchased online through the Department's bookshop at www.doir.wa.gov.au

Contents

Introduction 1
Geological history of the Pinjarra Orogen 3
Northampton and Mullingarra Complexes 3
Leeuwin Complex 5
Structure of the Leeuwin Complex 8
Northern Leeuwin Complex 8
D_1 structures 10
D_2 structures 10
D_3 structures 10
D_4 structures 10
D_5 structures 10
Southern Leeuwin Complex 10
D_1 structures 10
D_2 structures 11
D_3 structures 11
D_4 structures 11
Central Leeuwin Complex 11
Low-grade schist 11
Darling Fault Zone 11
Basement to the Perth Basin 13
Excursion localities 14
Darling Fault Zone 14
Locality 1: Harvey Weir Spillway 14
Locality 2: Roelands Granite Quarry 14
Southern Leeuwin Complex 15
Locality 3a: Skippy Rock (north) 15
Locality 3b: Skippy Rock (south) 15
Locality 4: Cape Leeuwin lighthouse 15
Locality 5: Sarge Bay 18
Locality 6: Ringbolt Bay 19
Locality 7: Northeast of Point Matthew 19
Locality 8a: Cosy Corner 19
Locality 8b: Elephant Rock 22
Locality 8c: Cape Hamelin 24
Central Leeuwin Complex 25
Locality 9: Cape Freycinet 25
Locality 10: Redgate Beach 25
Locality 11: Willyabrup Cliffs 25
Locality 12a: Moses Rock 27
Locality 12b: Honeycombs 27
Northern Leeuwin Complex 28
Locality 13: Sugarloaf Rock 28
Locality 14: Gull Rock 28
Locality 15: Shelley Beach, Bunker Bay 29
Acknowledgements 30
References 31

Figures

1. Map of southwestern Australia showing the locations of cities, towns, roads, and topographic features discussed in this field guide 1
2. Tectonic units of southwestern Australia 2
3. Parts of Australia, India, and Antarctica in a Gondwana fit, showing outcrop area and inferred extent of the Neoproterozoic to Cambrian Pinjarra Orogen 2
4. Features of the Darling Fault Zone 5
5. Outcrop map and field-trip locality map of the Leeuwin Complex 6
6. Map of structural relationships in the northern Leeuwin Complex from Dunsborough to Sugarloaf Rock 9
7. Schematic structural interpretation of the detailed structural map of the northern Leeuwin Complex depicted in Figure 6 10
8. Augen mylonite at Roelands Granite Quarry 14
9. Map of the southern Leeuwin Complex from Skippy Rock to Barrack Point 16

10. Detailed outcrop map of Skippy Rock showing the D_1/D_2 isoclinal folding of interleaved mafic bands and garnet-bearing felsic migmatite 17
11. Detailed map of the rock pavement southwest of Skippy Rock car park 18
12. Interlayered amphibolite and granite gneiss southwest of Skippy Rock car park 18
13. Pavement outcrop northeast of Cape Leeuwin lighthouse displaying boudinage of the pervasive steeply dipping S_1 foliation 18
14. Outcrop of garnet-bearing hornblende–plagioclase gneiss from the hinge region of an F_1 fold at Sarge Bay 19
15. Detailed map of pavement outcrops at Ringbolt Bay 20
16. Map of the Cosy Corner region from Foul Bay to Deepdene, showing the excursion localities, pertinent roads and tracks, and the extent of basement outcrops 21
17. Detailed outcrop map of a wave-cut platform at Cosy Corner that displays the blurred contact between garnet–hornblende gneiss and homogeneous granodiorite gneiss 22
18. Detailed outcrop map of Elephant Rock displaying amphibolite and granite gneiss folded into tight northwest-trending F_1 structures 23
19. Tight to isoclinal F_1 folds in an amphibolite layer at Elephant Rock 23
20. Interlayered amphibolite and granite gneiss with steep westerly dips at Cape Hamelin 24
21. Outcrop about 200 m east of Cape Hamelin illustrating D_3 buckling of an amphibolite layer that had been previously boudinaged during north–south D_1 extension 24
22. Isolated lens of folds within a garnet-bearing granite gneiss at Cape Freycinet 25
23. Map of the northern Leeuwin Complex showing Localities 11 to 15 and the extent of basement outcrop 26
24. Recumbent, tight to isoclinal fold in an amphibolite layer in granite gneiss at Willyabrup Cliffs 27
25. Plagioclase–hornblende reaction rims around garnet in an amphibolite horizon at Willyabrup Cliffs 27
26. Detailed outcrop map of the D_2 Sugarloaf Antiform, outcropping on the peninsula directly south of Sugarloaf Rock 28
27. Unconformity at Shelley Beach, Bunker Bay 29

Structure and tectonics of the Leeuwin Complex and Darling Fault Zone, southern Pinjarra Orogen, Western Australia — a field guide

by

D. P. Janssen[1], A. S. Collins[1], and I. C. W. Fitzsimons[1]

Introduction

This field guide has been prepared as an aid for those attending the excursion to the Leeuwin Complex and Darling Fault Zone, held as part of the Geological Society of Australia's Specialist Group in Tectonics and Structural Geology Field Meeting, Kalbarri 2003. It describes some of the best exposed outcrops of the Pinjarra Orogen, which preserve evidence for the tectonic evolution of Australia's western margin throughout the Neoproterozoic and into the Cambrian.

The Darling Scarp, at the western edge of the Darling Range, is arguably the dominant topographic feature of Western Australia, passing just to the east of Perth and the Swan Coastal Plain (Fig. 1), and extending for hundreds of kilometres north and south. It is the current-day surface expression of the Darling Fault, which itself dominates geological maps and geophysical images of the State (Fig. 2). The Darling Fault marks the western edge of the Australian craton. To its east lie the ancient Yilgarn Craton and the Proterozoic Capricorn and Albany–Fraser Orogens. To its west lie a number of Proterozoic to Cambrian gneissic inliers draped by Phanerozoic sedimentary rocks of the Perth and Southern Carnarvon Basins. The present morphology of the Darling Fault reflects Mesozoic rifting during the opening of the Indian Ocean, but this extensional structure has exploited a much older Precambrian transcurrent shear zone known as the Darling Fault Zone. This crustal-scale shear zone at the craton margin and the outboard gneissic inliers are all components of the Pinjarra Orogen, which records 500 million years of Neoproterozoic to Cambrian tectonic activity associated with the assembly of Gondwana (Fig. 3).

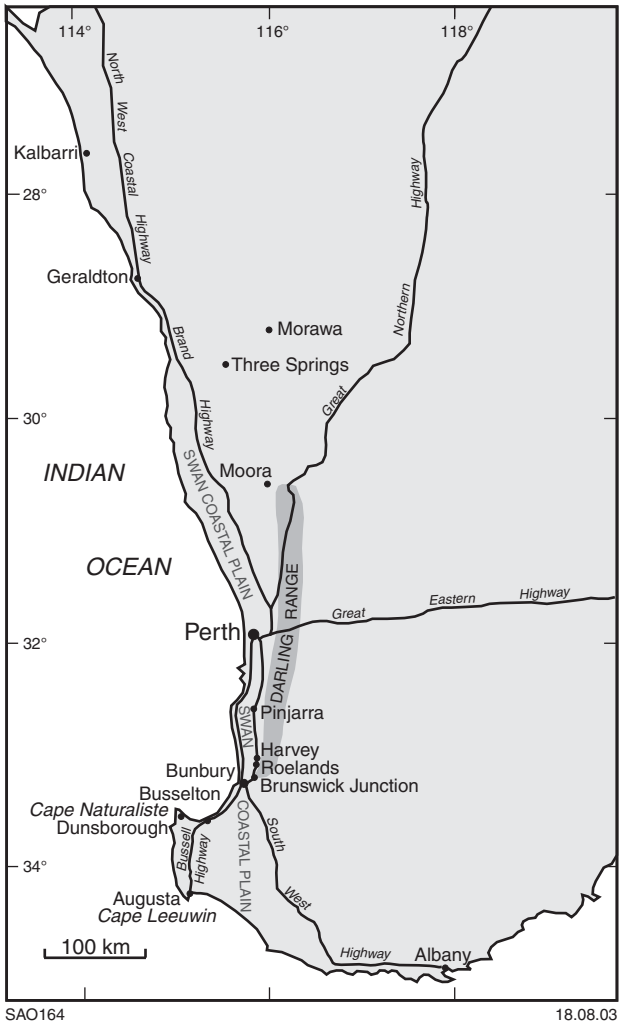

Figure 1. Map of southwestern Australia showing the locations of cities, towns, roads, and topographic features discussed in this field guide

[1] Tectonics Special Research Centre, Department of Applied Geology, Curtin University of Technology, PO Box U1987, Perth, W.A. 6845.

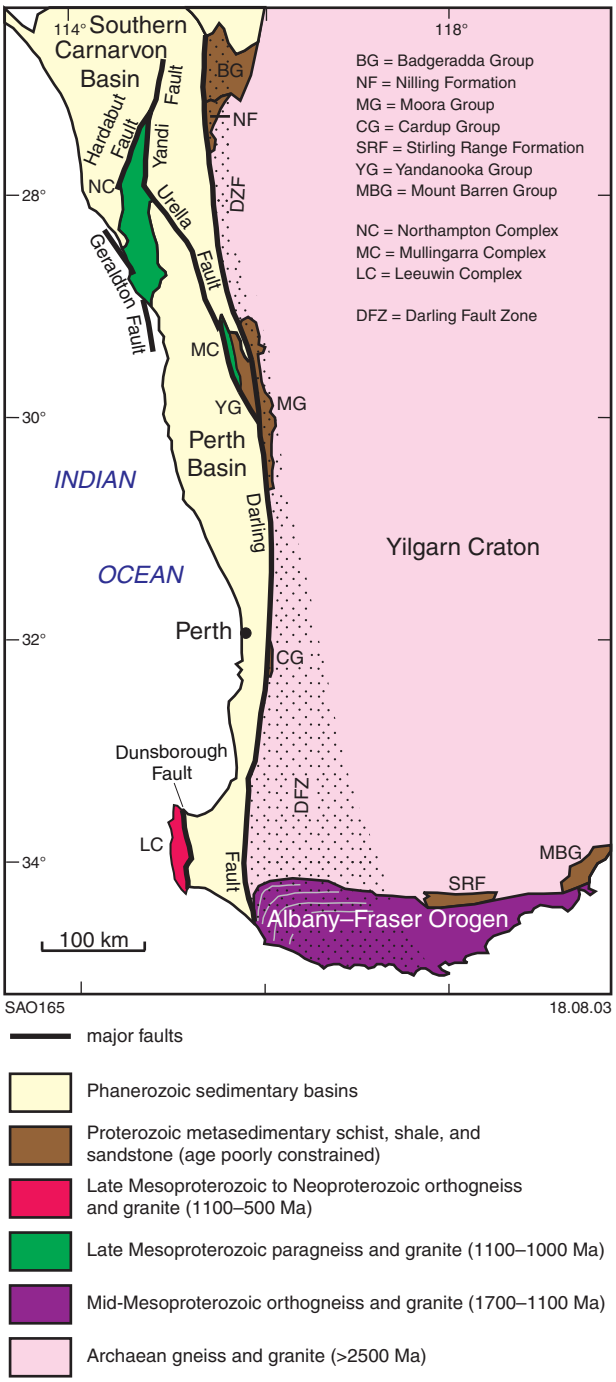

Figure 2. Tectonic units of southwestern Australia

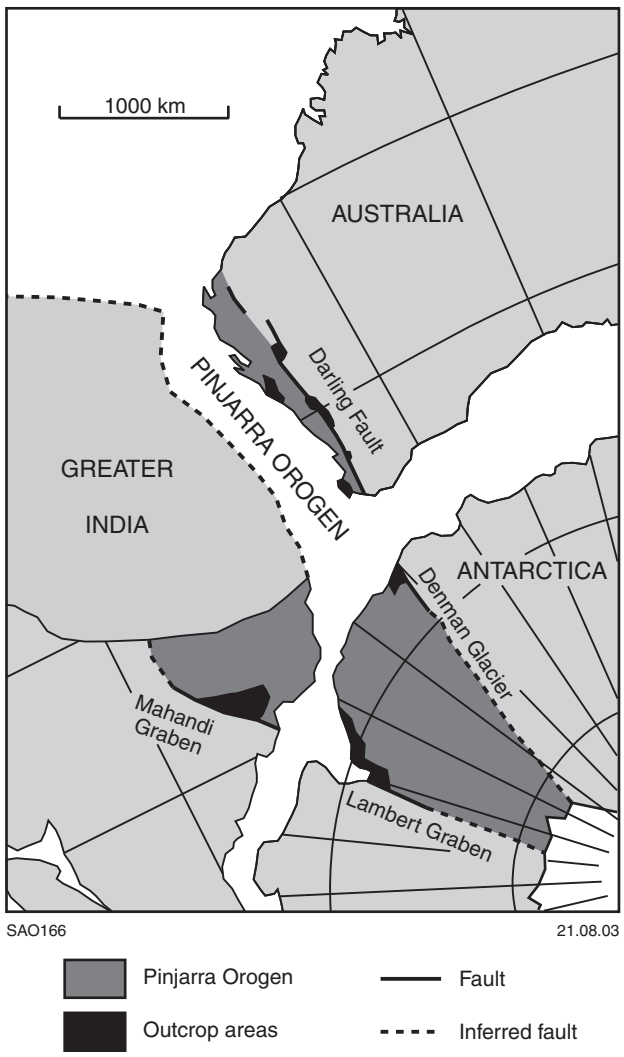

Figure 3. Parts of Australia, India, and Antarctica in a Gondwana fit, showing outcrop area and inferred extent of the Neoproterozoic to Cambrian Pinjarra Orogen. Its eastern margin has been reactivated by the Mesozoic Darling Fault in Australia and a similar fault inferred to lie beneath the Denman Glacier in Antarctica. Its western margin has been reactivated by the Mesozoic Lambert–Mahanadi graben system, and much of the Indian segment of the orogen was subducted with Greater India beneath Tibet

In contrast to the much-studied eastern margin of the Australian craton, the history of the Pinjarra Orogen is poorly understood. This reflects to some degree its poor preservation. Although the Pinjarra Orogen in Western Australia is only a small part of a much larger Neoproterozoic orogen that extends into Australia's Gondwana neighbours (Fig. 3), much of the Indian segment has been subducted beneath Tibet during the Himalayan collision or buried by the Bengal Fan and alluvial deposits of the Ganges River, whereas the Antarctic segment is largely covered by the ice sheet. Even in Western Australia, much of the orogen is concealed beneath Phanerozoic basins. This field guide is concerned with the evolution of the best exposed part of the Pinjarra Orogen — the Leeuwin Complex — and its relationships with the craton, which are preserved within the Darling Fault Zone. Previous field guides to this region include those of Myers (1994), Nelson (1995), and Wilde and Nelson (2001).

The area covered in this excursion represents the extreme southwestern tip of Australia (Fig. 1). Sporadic outcrops of the Darling Fault Zone between the towns of Harvey and Brunswick Junction are at the edge of some of Australia's best agricultural land, renowned for dairy, beef, and citrus products. This region also has substantial deposits of bauxite and titanium-rich mineral sands. Farther south, the coastal outcrops of the Leeuwin Complex,

between the towns of Dunsborough and Augusta, are incorporated within the Leeuwin–Naturaliste National Park. This region has a spectacularly rugged coastline, pristine sandy beaches, limestone caves, karri forests, and superb local wines. These regions figure prominently in the early history of European exploration and settlement in Western Australia, and the interactions between Europeans and the Aboriginal people. Many of the sites that will be visited are environmentally sensitive and protected. Rock samples may not be taken from any sites in the National Park without the prior arrangement and approval of the Western Australian Department of Conservation and Land Management (CALM).

Despite being one of Australia's more benign regions, fieldwork in the southwest does carry a number of risks. The coastline can be subject to large swells and king waves, some beaches have dangerous rips and undertows, coastal limestone cliffs are fragile with dangerous overhangs, and rounded gneissic rock outcrops can be extremely slippery after storms or heavy rainfall. Venomous western tiger snakes and dugites are present, but rarely seen.

Geological history of the Pinjarra Orogen

The current western margin of the Yilgarn Craton and Albany–Fraser Orogen is marked by the Darling Fault, which is at least 1500 km long with a record of normal displacement during Gondwana breakup. There is widespread evidence, summarized below, that this Phanerozoic structure has reactivated a much older north-trending tectonic boundary associated with Proterozoic to Cambrian tectonic activity at 1100–1000, 800–650, and 550–500 Ma. This region of late Mesoproterozoic to Cambrian tectonism along the western margin of Australia was first referred to as the Darling Mobile Belt (Glikson and Lambert, 1973; Harris, 1994a), but was later renamed the Pinjarra Orogen (Myers, 1990a), and the latter name is used here. There is in fact no basement outcrop at Pinjarra — a small town known for the Battle of Pinjarra in 1834, a bloody and one-sided clash that signified the end of Western Australian isolation from the influence of the western world. It is, however, a fitting name for an orogen that records the processes leading up to the incorporation of Australia in the Gondwana super-continent. The orogen has also been a major influence on the geological evolution of Western Australia throughout the Phanerozoic. Basement faults and shear zones of the Pinjarra Orogen have controlled the structural evolution of the overlying basins (Harris, 1994b; Harris et al., 1994), and the orogen has also provided much of the detritus in these basins (Sircombe and Freeman, 1999; Cawood and Nemchin, 2000).

The identification of multiple tectonic events in the Pinjarra Orogen has led to some confusion in terminology. Myers et al. (1996) used the term Proto-Pinjarra Orogeny to refer to 1100–1000 Ma events, and suggested that the term Pinjarra Orogeny be reserved for Neoproterozoic to Cambrian tectonism, culminating at 550–500 Ma. Wilde (1999) argued that the term Pinjarra Orogeny should be restricted to the 1100–1000 Ma events, since it was the identification of these events by preliminary geochronological investigations that first established the presence of a distinct Proterozoic orogen along the western margin of Australia. However, as discussed below, it is likely that the 1100–1000 Ma terranes were accreted to their present position sometime during the Neoproterozoic. Following Fitzsimons (2003), we use the term Pinjarra Orogen to describe the belt of terranes accreted to the western margin of the Australian craton during the Neoproterozoic and Cambrian, and also the rocks of the craton margin affected by these accretion events. The older events preserved by some of the outboard terranes are likely to be unrelated to this accretion process, and their tectonic setting and original geographic location remain poorly understood.

The Pinjarra Orogen is largely concealed by the Phanerozoic Perth and Southern Carnarvon Basins, and evidence for its evolution comes from three main sources (Fig. 2):

- fault-bound Proterozoic gneissic inliers exposed as the Northampton, Mullingarra, and Leeuwin Complexes west of the Darling Fault;
- low-grade metasedimentary schists of assumed Proterozoic age that outcrop on either side of the Darling Fault;
- reworked margins of the Yilgarn Craton and Albany–Fraser Orogen immediately east of the Darling Fault, known as the Darling Fault Zone (Myers, 1990a).

Northampton and Mullingarra Complexes

The Northampton and Mullingarra Complexes are the two northernmost gneissic inliers of the Pinjarra Orogen, located about 300–400 km north of Perth (Fig. 2). The Northampton Complex is the larger of the two, and forms a horst exposed over an area of 100 × 30 km immediately east of Geraldton and Kalbarri. It is bound by numerous faults, including the Hardabut Fault in the northwest, the Yandi Fault in the northeast, and the Geraldton Fault in the southwest. The Mullingarra Complex is exposed as a narrow 60 km-long strip of low-lying hills immediately east of the Urella Fault and west of the town of Three Springs. It is unconformably overlain along its eastern margin by the low-grade metasedimentary Yandanooka Group of inferred Proterozoic age.

These complexes are dominated by psammitic paragneiss, with conformable lenses of pelite, quartzite, and mafic gneiss, and subordinate intrusive rocks (Peers, 1971, 1975; Myers, 1990a). Initial investigations by Hocking et al. (1982), Playford et al. (1970), and Baxter and Lipple (1985) distinguished the main rock units depicted and described in 1:250 000 map sheets and explanatory notes of the Geological Survey of Western Australia (GSWA). The oldest rock identified in these two complexes is an unmetamorphosed monzogranite in the Mullingarra Complex, in faulted contact with overlying metasedimentary gneiss, with a sensitive high-mass resolution ion microprobe (SHRIMP) U–Pb zircon

crystallization age of 2181 ± 10 Ma (Cobb, 2000; Cobb et al., 2001). SHRIMP U–Pb zircon studies of detrital zircon from psammitic rocks in both the Northampton and Mullingarra Complexes (Bruguier et al., 1999; Cobb, 2000; Cobb et al., 2001) have identified consistent age distributions, with major populations at 1900–1600 and 1400–1150 Ma, indicating that they were eroded from the same source rocks and belong to the same sedimentary package. The youngest detrital grain was dated at 1113 ± 26 Ma, providing a maximum depositional age. These detrital age populations closely match the age of exposed basement rocks in the Albany–Fraser Orogen, and are thought to have been eroded from them (Kriegsman et al., 1999; Fitzsimons, 2003).

Blight and Barley (1981) estimated that metamorphic temperature and pressure in the Northampton Complex reached 600–800°C and 5–7 kbar. Later work has shown that the sedimentary rocks were pervasively deformed and metamorphosed to granulite facies in the Northampton Complex (6 kbar, 850°C; Kriegsman and Hensen, 1998) and to amphibolite facies in the Mullingarra Complex (6 kbar, 670°C; Cobb et al., 2000, 2001). Metamorphic assemblages in pelitic bulk compositions include garnet–cordierite–sillimanite–K-feldspar in the Northampton Complex and garnet–sillimanite–muscovite–quartz in the Mullingarra Complex. The timing of metamorphism was initially constrained by Rb–Sr muscovite ages of 1000 and 1120 Ma from the Northampton and Mullingarra Complexes (Wilson et al., 1960), and a Rb–Sr whole-rock isochron age of 1040 ± 50 Ma for granulites from the Northampton Complex (Compston and Arriens, 1968). These ages have been refined by SHRIMP U–Pb analyses of metamorphic zircons that yielded ages of 1079 ± 3 and 1079 ± 32 Ma for the Northampton and Mullingarra Complexes respectively (Bruguier et al., 1999; Cobb, 2000; Cobb et al., 2001). The Northampton Complex was intruded by a granite pluton at 1068 ± 13 Ma (Bruguier et al., 1999) and then folded about shallow northwesterly trending axes, with similar structures identified in the Mullingarra Complex. This tectonic episode concluded with pegmatite dyke emplacement, dated in the Northampton Complex at 989 ± 2 Ma (Bruguier et al., 1999).

Later tectonism in the Northampton Complex was marked by the emplacement of north-northeasterly trending dolerite dykes with a K–Ar age of about 750 Ma (Embleton and Schmidt, 1985), which were initially correlated with the Muggamurra dyke swarm of the Yilgarn Craton (Fig. 4a), but have palaeomagnetic poles indistinguishable from the 755 ± 3 Ma Mundine Well dyke swarm of the Pilbara Craton (Wingate and Giddings, 2000). The orientations of these dykes and later brittle–ductile shear zones are consistent with north–south dextral wrenching (Byrne and Harris, 1993). They are cut by sinistral, south-southeasterly trending, greenschist- to amphibolite-facies shear zones that developed at about 550 Ma, according to K–Ar data from dykes adjacent to these shear zones (Embleton and Schmidt, 1985). There are no reports of mafic dykes or sinistral shear zones cutting the Mullingarra Complex, although this could reflect poor outcrop rather than a significant difference in geological history.

Late Mesoproterozoic tectonism in the Northampton and Mullingarra Complexes has been widely regarded as evidence for a 'Grenville-age' collisional suture between Australia and India, since they lie between these two continents in Gondwana reconstructions (Myers et al., 1996; Bruguier et al., 1999). However, there is increasing geological and palaeomagnetic evidence that India and Australia did not attain their adjacent Gondwana positions until the late Neoproterozoic (Fitzsimons, 2000, 2003; Torsvik et al., 2001; Powell and Pisarevsky, 2002; Pisarevsky et al., 2003). Petrological and geochronological evidence that sedimentary protoliths in the Northampton and Mullingarra Complexes were buried to depths of 20 km within 50 m.y. of their erosion from the Albany–Fraser Orogen is consistent with collision between Western Australia and an unidentified continental block at about 1100 Ma, but that continent is unlikely to be India. Fitzsimons (2002, in press) suggested that the colliding continent could have been the Kaapvaal–Zimbabwe Craton of southern Africa, on the basis of similarities in detrital and metamorphic zircon ages between paragneisses of the Pinjarra Orogen and metasedimentary rocks exposed adjacent to the Kaapvaal Craton. This suggestion is also supported by available palaeomagnetic data (Pisarevsky et al., 2003).

Whatever the identity of the colliding continent, an important question is whether the Northampton and Mullingarra Complexes were metamorphosed in their present-day locations, or were transported as a result of the younger tectonic events recorded in the Pinjarra Orogen — a possibility first acknowledged by Myers (1990a, 1993). Cobb et al. (2001) and Fitzsimons (2003) adopted this latter model and argued that the Northampton and Mullingarra Complexes are allochthonous blocks transported to their present location during the Neoproterozoic. Evidence for an allochthonous origin includes an apparent lack of pervasive 1080 Ma tectonism at the edge of the Yilgarn Craton adjacent to the Mullingarra Complex. This part of the Yilgarn Craton preserves Palaeoproterozoic Rb–Sr biotite ages (see **Darling Fault Zone**; Fig. 4b) even though the Mullingarra Complex is only 15 km from the craton margin. Furthermore, the undeformed Palaeoproterozoic granite body in the Mullingarra Complex must have been juxtaposed against the adjacent gneiss after 1080 Ma metamorphism, providing conclusive evidence for significant post-metamorphic tectonic displacement. The identification of only four Archaean grains out of 132 detrital grains analysed from three samples of Northampton and Mullingarra paragneiss (Bruguier et al., 1999; Cobb, 2000; Cobb et al., 2001) is also difficult to reconcile with deposition immediately adjacent to the Yilgarn Craton, but up to 800 km from likely source rocks in the Albany–Fraser Orogen.

Fitzsimons (2001, 2003) argued that the Northampton and Mullingarra Complex sediments were deposited south of their present position some time between 1130 and 1080 Ma, perhaps south of the watershed in the Albany–Fraser mountains to account for the lack of Yilgarn Craton detritus, and then buried and metamorphosed at 1100–1050 Ma during continental collision. These rocks were then translated northward by as much as 800 km during dextral strike-slip movement to reach their present-day

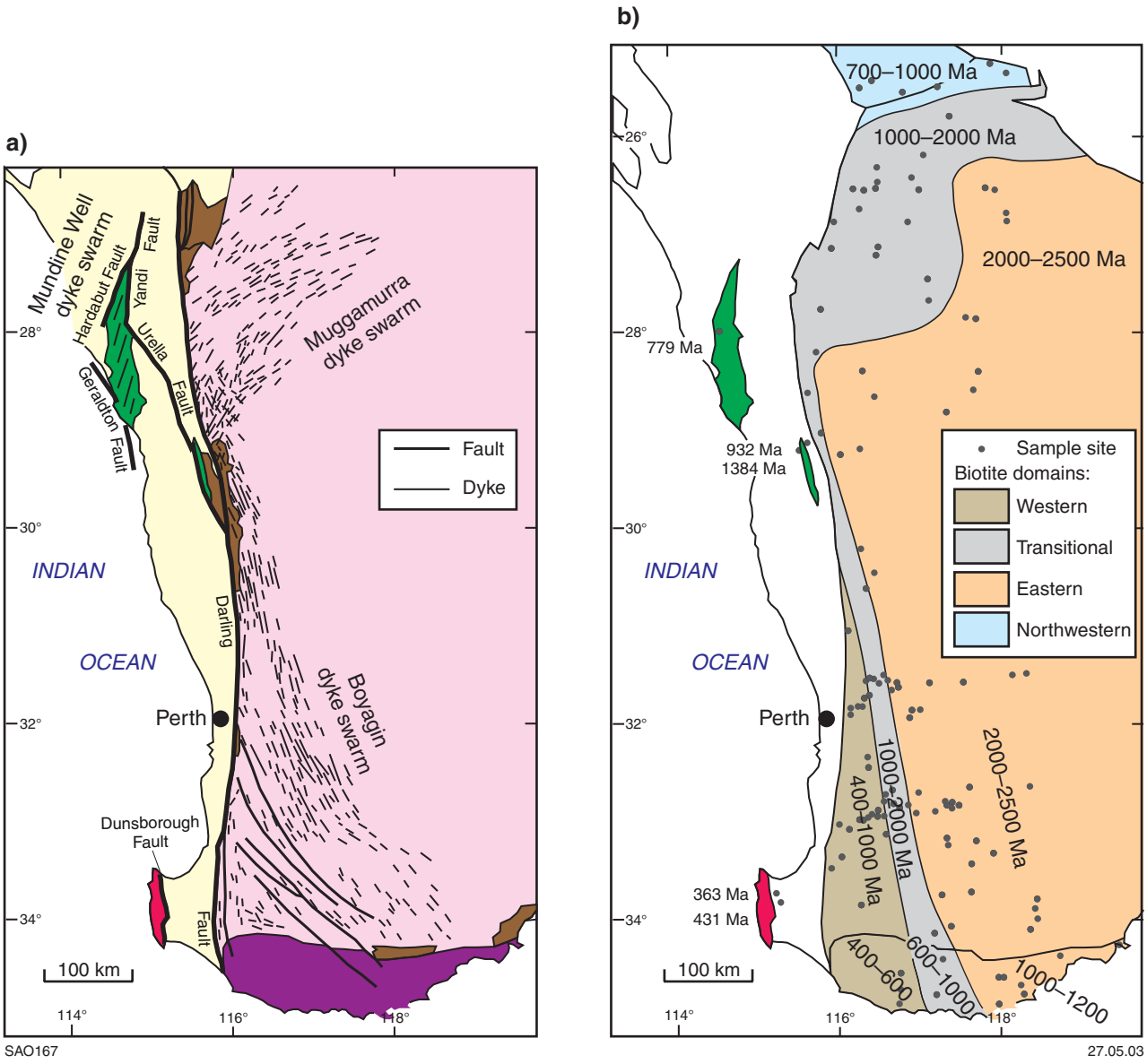

Figure 4. Features of the Darling Fault Zone (tectonic unit colours as for Figure 2): a) the Mundine Well, Muggamurra, and Boyagin dyke swarms, and major faults cutting the Yilgarn Craton, Albany–Fraser Orogen, some of the low-grade schistose metasedimentary rocks, and the Northampton Complex; b) the distribution of Rb–Sr biotite ages in southwest Australia, showing the biotite domains as defined for the Yilgarn Craton by Libby and de Laeter (1998) and Libby et al. (1999). Note that the gneissic inliers of the Pinjarra Orogen have colours after Figure 2 and are not ascribed to a biotite domain

position adjacent to the northwest Yilgarn Craton. This sense of movement is consistent with the structural evidence for dextral wrenching of the Northampton Complex during dyke emplacement and brittle–ductile deformation (Byrne and Harris, 1994). Palaeomagnetic data require that the Northampton Complex has not moved significantly relative to the Australian craton since mafic dyke emplacement at 755 Ma (Wingate and Giddings, 2000), implying that the dykes and brittle–ductile shear zones in this complex represent the final stages of dextral movement as the Northampton Complex was accreted to the northwestern Yilgarn Craton.

Leeuwin Complex

The Leeuwin Complex is exposed in the far southwest of Western Australia, about 200 km south of Perth (Fig. 2), as a narrow coastal ridge between Cape Naturaliste in the north and Cape Leeuwin in the south. Unlike the two northern inliers, it is composed predominantly of granitic orthogneiss, locally overlain by Tertiary laterite, sand, and the Quaternary Tamala Limestone. Along its eastern margin it is bound by the Dunsborough Fault, which runs between the towns of Dunsborough and Augusta (Fig. 5).

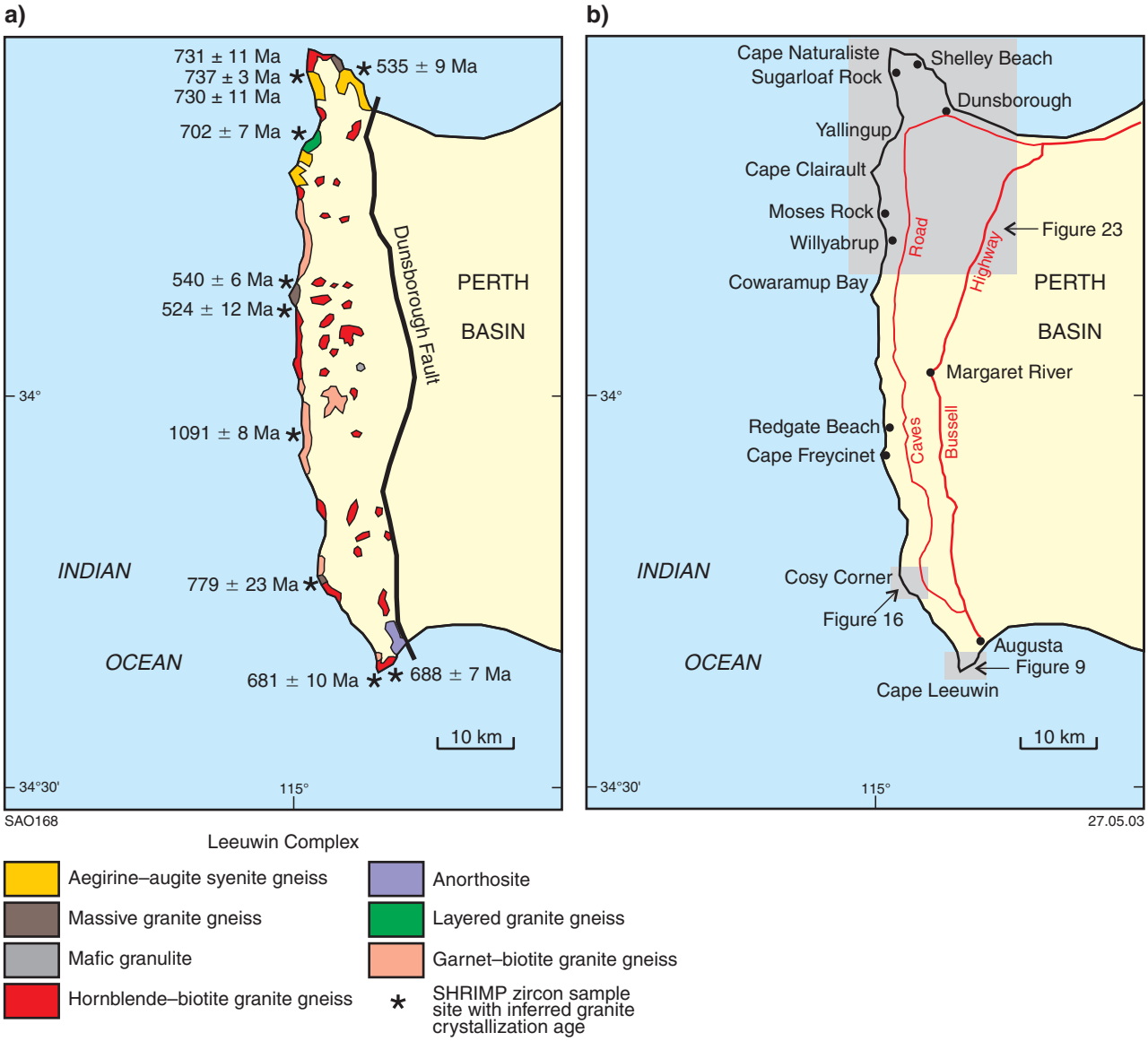

Figure 5. **a) Map of the Leeuwin Complex showing the approximate outcrop extent of the main lithologies distinguished by Wilde and Murphy (1990), and the sampling sites for rocks dated by Nelson (1996, 1999, 2002) and Collins (in press) using SHRIMP U–Pb zircon techniques, annotated with the igneous protolith crystallization ages inferred in each case; b) map showing the approximate positions of the field-trip localities and of more-detailed location maps presented elsewhere in this field guide**

The geology of this area was first described during the Baudin expedition of 1800–04 (Péron and Freycinet, 1807–1816), when the mineralogist Dupuch reported 'stratified' granite from the Cape Naturaliste region. This was taken as supporting evidence for the Neptunist theory that granite was a sedimentary rock, and regarded as one of the few scientific successes of an otherwise disappointing study of the region.

Although identified in the early 20th Century as a separate tectonic block (Saint-Smith, 1912), it was not until early Rb–Sr whole-rock studies yielded a 670 ± 25 Ma Neoproterozoic isochron age (Compston and Arriens, 1968) that the distinct magmatic, deformational, and metamorphic history of the region was appreciated. More-recent dating in the Leeuwin Complex using a range of techniques has confirmed the presence of the 700–670 Ma plutons that distinguish this area from all other gneissic regions of Western Australia, and has also identified several other magmatic episodes that range from late Mesoproterozoic to Cambrian in age. Dredge samples taken from the submarine Naturaliste Plateau (Beslier et al., 2001), more than 500 km west of the Leeuwin–Naturaliste coast, gave Ar^{40}–Ar^{39} ages of 508.2 ± 1 (amphibole), 494 ± 1 (amphibole), and 507.7 ± 1 Ma (biotite), demonstrating that the exposed Leeuwin Complex is but a small onshore outcrop of an extensive region of Neoproterozoic to Cambrian orogenesis (Borissova, 2002).

Geological mapping of the Leeuwin Complex has been largely restricted to either broad-scale lithological mapping (Lowry, 1967; Wilde and Murphy, 1990;

Murphy, 1992), or detailed outcrop-scale mapping to unravel specific relationships or processes (Myers, 1990a,b, 1994; Harris, 1994a, 2003; Hopgood and Bowes, 1995). The only detailed kilometre-scale maps are those of Kay (1958), Andrews (1967), and Stolze (2000), who produced maps of the Cape Naturaliste, Cape Leeuwin, and Yallingup–Honeycombs regions, respectively, as part of their Honours theses. Many of these studies have attempted to construct a simple classification scheme for the lithologies observed in the Leeuwin Complex, but with limited success given the difficulty of devising such a scheme for a variety of felsic orthogneisses with subtle variations in mineralogy, fabric, chemistry, and protolith age.

Local lithological schemes include those of Carroll (1940) and Andrews (1967) for Cape Leeuwin, and Kay (1958) for Cape Naturaliste. Carroll (1940) described four types of gneiss from Cape Leeuwin: a banded hornblende–plagioclase rock (zebra gneiss), a massive brown rock (Barrack Point gneiss), a hornblende pegmatite rock (basic series), and a pink feldspar–hornblende gneiss (Leeuwin gneiss). Andrews (1967) divided the same rocks into banded hornblende–plagioclase amphibolite, acid granulites of various modal compositions, wisp-banded granulite, and basic granulite. Kay (1958) classified the gneisses around Cape Naturaliste by their mafic mineral assemblage, and erected the following subdivisions: hornblende granulite, hornblende–orthopyroxene–clinopyroxene granulite, hornblende–clinopyroxene granulite, clinopyroxene granulite, sodic pyroxene granulite, fayalite granulite, biotite granulite, and garnet granulite.

The first attempt to devise a lithological scheme for the Leeuwin Complex as a whole was a result of mapping by Horwitz, Gemuts, and Lowry for GSWA (Lowry, 1967). Lowry mapped the Quaternary deposits, whereas the gneisses were mapped by Horwitz and Gemuts, who erected four subdivisions based on field relationships: coarse-grained granulite, basic granulite, medium-grained granulite, and granite gneiss. The last of these was considered to be the youngest lithology and to have intruded the other rocks concordant to locally discordant sheets. This scheme has similarities with that of Myers (1994), who divided the Leeuwin Complex into the Cowaramup Gneiss and Hamelin Granite, based on the degree of deformation. He defined the older Cowaramup Gneiss as a strongly deformed and metamorphosed composite of interleaved anorthosite, leucogabbro, gabbro, sheets of granite, and pegmatite veins. The Hamelin Granite forms large sheet-like bodies that vary in texture from coarse porphyritic, to coarse even grained, to fine even grained. These sheets were emplaced into the older gneisses and associated with the intrusion of dolerite dykes. A different approach was taken by Wilde and Murphy (1990) and Murphy (1992), who subdivided the Leeuwin Complex on the basis of mineralogy (Fig. 5a), and did not attempt to construct a relative chronology. They identified layered plagioclase–hornblende gneiss, massive mafic gneiss, and six types of felsic gneiss:

- Type 1 is a layered, two-feldspar–garnet–biotite gneiss;
- Type 2 is a layered, two-feldspar–pyroxene/hornblende–biotite gneiss;
- Type 3 is massive to layered, alkali feldspar – Na/Fe-pyroxene/amphibole gneiss;
- Type 4 is a layered, alkali feldspar – biotite gneiss;
- Type 5 is a massive, two-feldspar gneiss;
- Type 6 is a massive, two-pyroxene felsic granulite.

All of these have similar geochemistry, apart from Type 6 gneisses, suggesting that much of the Leeuwin Complex was derived from a similar granitic protolith (Wilde and Murphy, 1990).

Wilde and Murphy (1990) obtained the first U–Pb zircon ages for the Leeuwin Complex of 570–550 Ma, which are interpreted as igneous crystallization ages of orthogneiss protoliths, but T_{DM} (depleted mantle) Nd model ages of 1600–1100 Ma* (McCulloch, 1987; Fletcher and Libby, 1993; Black et al., 1992) indicate that much of the complex has a significantly older history. This was confirmed by U–Pb SHRIMP zircon data (Fig. 5a), which revealed that the orthogneiss protoliths were emplaced in three broad stages at 1100–1000, 800–650, and 550–500 Ma (Nelson, 1996, 1999, 2002; Collins, in press). Garnet-bearing augen gneiss from Redgate Beach in the central Leeuwin Complex has yielded the oldest zircon crystallization ages of 1091 ± 8 and 1091 ± 17 Ma, whereas various types of hornblende-bearing gneiss were emplaced at several localities over an extended period from 800 to 650 Ma. The relationship between these two protolith groups is unknown, and no samples have yielded evidence of both events. In contrast, the youngest magmatic pulse at 550–500 Ma seems to have affected all other lithologies. One of the upper Mesoproterozoic protoliths at Redgate Beach contained a concordant zircon at 531 ± 64 Ma, indicating an overprint of some sort at this time (Nelson, 1999). Several samples from Sugarloaf Rock in the northwestern Leeuwin Complex contain complicated mixtures of 750–520 Ma zircon populations interpreted in terms of a 540–520 Ma overprint on a 750–700 Ma protolith (Nelson, 2002; Collins, in press). Unlike the older gneisses, hornblende–biotite granite and aegirine-augite syenite rocks emplaced at 540 ± 6 and 535 ± 9 Ma are not compositionally banded, but are still foliated and folded, suggesting that at least some of the deformation occurred after their intrusion. An unfoliated hornblende–biotite monzogranite dyke emplaced at 524 ± 12 Ma provides a possible minimum age for this latter deformation (Nelson, 1996).

Mafic lithologies form boudinaged foliation-parallel sheets throughout the Leeuwin Complex, and are typically interpreted as transposed mafic dykes (Myers, 1990a; Simons, 2001). They preserve upper amphibolite- or granulite-facies mineral assemblages, and provide the best evidence for metamorphic conditions in the complex. Wilde and Murphy (1990) described a prograde transition from amphibolite facies in the south to granulite facies in the north, and attributed a lack of garnet in mafic rocks to relatively low-pressure conditions. However, Myers

* To enable comparison of different Sm–Nd datasets, all Nd isotope ratios have been renormalized (if necessary) to $^{146}Nd/^{144}Nd = 0.7219$, and quoted Nd model ages recalculated relative to a depleted mantle with present-day composition of $^{143}Nd/^{144}Nd = 0.51316$ and $^{147}Sm/^{144}Nd = 0.225$, assuming a decay constant of 6.54×10^{-12} and the linear e_{Nd} growth model of Goldstein et al. (1984).

(1994) argued that peak conditions reached granulite facies throughout the complex, and that amphibolite-facies assemblages were retrograde. The timing of peak metamorphism is difficult to constrain since metamorphic assemblages are best preserved by mafic rocks, whereas the best geochronological data come from accessory minerals in the granite gneisses. Nelson (1995) argued that the age of peak granulite-facies metamorphism in the Leeuwin Complex was constrained by a cluster of zircon ages at 630–600 Ma in a granite sample from Cosy Corner in the southwest Leeuwin Complex, with a protolith crystallization age of 779 ± 23 Ma. He further suggested that subsequent amphibolite-facies metamorphism must have post-dated the 540 ± 6 Ma emplacement of alkali granite at Cowaramup Bay in the central Leeuwin Complex, which is now a gneiss with amphibolite-facies hornblende–biotite assemblages. Collins (in press) noted, however, that the 630–600 Ma ages could be partly reset and only give a maximum constraint on the timing of metamorphism, and he believed the evidence from Sugarloaf Rock for an overprint at 530–520 Ma (Nelson, 2002; Collins, in press) to be a better constraint on peak metamorphism in the complex as a whole. This is consistent with the SHRIMP U–Pb age of 536 ± 21 Ma obtained by Simons (2001) for zircons from a hornblende–two-pyroxene mafic granulite gneiss at Shelley Beach. Simons (2001) argued that this age gave the time of igneous crystallization of the precursor mafic dyke, and thus a maximum age for granulite-facies metamorphism. However, the abundance of locally derived leucosome within this unit suggests that the zircon could actually have grown during partial melting and thus give the age of peak metamorphism. Whatever the interpretation, these data imply that granulite-facies conditions were attained at or after 540 Ma, at least in the northern Leeuwin Complex.

The geochronological evidence for a prolonged multi-stage magmatic history is difficult to reconcile with a reported lack of significant geochemical variation (Wilde and Murphy, 1990), but reassessment of published geochemical data (Wilde and Murphy, 1990; Nelson, 1995; Wilde, 1999) by Collins and Fitzsimons (2001) has revealed significant differences in trace-element composition between orthogneiss protoliths. Precursors of the garnet–biotite orthogneiss emplaced at 1090 Ma have trace-element concentrations consistent with a syncollisional origin, according to standard geochemical discrimination diagrams, and do not have A-type characteristics. Conversely, 800–650 and 540–520 Ma protoliths are typical A-type granites, and although the former have trace-element concentrations typical of a within-plate origin, the latter have concentrations that show a wide scatter across several fields on discrimination diagrams. Fitzsimons (2003) argued that 1090 Ma magmatism in the Leeuwin Complex was probably related both spatially and genetically to 1080 Ma metamorphism of the Northampton and Mullingarra Complex paragneisses. Although not conclusive, geochemical evidence for a collisional setting in the Leeuwin Complex at 1090 Ma is consistent with burial and metamorphism of Northampton and Mullingarra Complex sediments at 1080 Ma to depths of 20 km. There is little evidence for the tectonic setting of 800–650 Ma magmatism, but it is the same age as the inferred trans-current transport and accretion of the Northampton and Mullingarra Complexes to the Yilgarn Craton. It also corresponds to a time period widely believed to be associated with the breakup of Rodinia, the supercontinent believed to have existed during the late Mesoproterozoic to early Neoproterozoic (Powell et al., 1994; Pisarevsky et al., 2003).

Potential settings suggested for the youngest phase of magmatism in the Leeuwin Complex (540–520 Ma) have been greatly influenced by the relatively alkaline character of these rocks, which contain minerals such as aegirine-augite and arfvedsonite. Wilde and Murphy (1990) noted that the emplacement of such alkaline granites was consistent with the Leeuwin Complex being in a continental rift environment at 550–500 Ma. Harris (1994a) argued that this time period was characterized by sinistral transcurrent displacement along the Darling Fault Zone, and suggested that local extension in the Leeuwin Complex was generated within an extensional jog of the strike-slip system. It now seems likely that the dominant sinistral component of tectonic transport at 550–500 Ma was in fact due to the oblique collision of India with Australia along the Pinjarra Orogen at this time (see **Darling Fault Zone**).

Structure of the Leeuwin Complex

Until very recently, there had been no attempt to develop a comprehensive model for the structural evolution of the Leeuwin Complex. Instead the emphasis had been on geochronology linked to orthogneiss mineralogy and geochemistry, and the lack of structural framework has hindered the interpretation of the complex. Of particular importance is the need to establish to what degree the different-aged orthogneiss protoliths share a common structural history, and to identify the nature and age of any structural boundaries that might exist between them. A structural mapping program in the northern Leeuwin Complex has been completed by Collins (in press). Similar work at the southern end of the complex is ongoing, but a preliminary structural model is presented in this field guide. Structures in both of these areas are dominated by upright north-trending folds with gently plunging hinges. The structure of the central Leeuwin Complex is less well studied, but preliminary data indicate that flat-lying high-strain foliations are dominant.

Northern Leeuwin Complex

The large-scale structure of the northern Leeuwin Complex was initially resolved by Kay (1958), who identified two stages of deformation (D_1 and D_2), the first forming recumbent isoclinal folds, and the second forming kilometre-scale, north-plunging asymmetric folds that dominate the structure of the region. More-detailed mapping by Collins (in press) built on Kay's pioneering work and identified a further two stages of folding (D_3 and D_4) that deform the earlier structures and fabrics (Figs 6 and 7). The following descriptions are based on the work of Collins (in press).

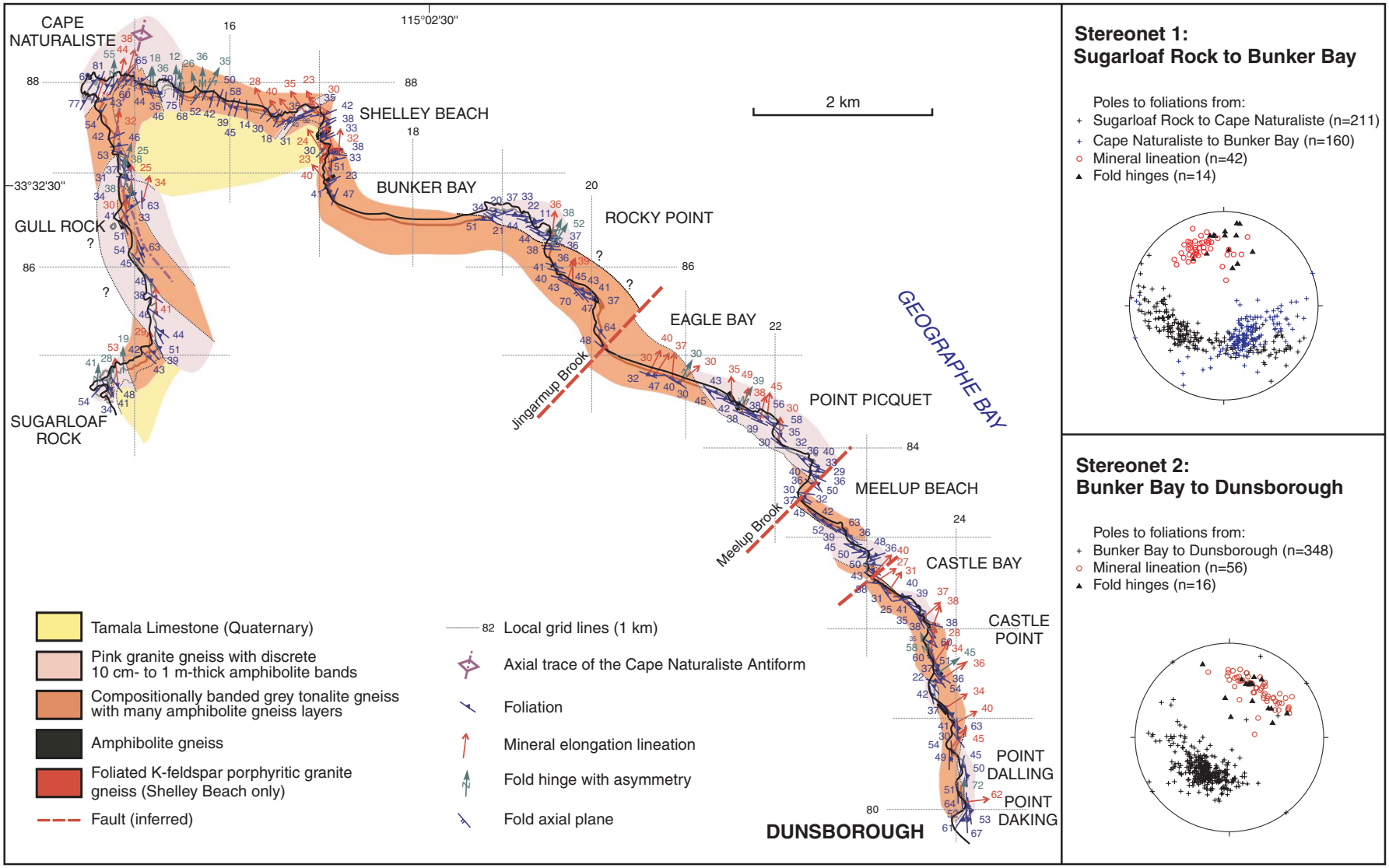

Figure 6. Map of structural relationships in the northern Leeuwin Complex from Dunsborough to Sugarloaf Rock (after Collins, in press). Structural data are presented in two stereonets (lower hemisphere, equal-area projections). Stereonet 1 portrays foliations between Sugarloaf Rock and Bunker Bay, and illustrates that data collected between Cape Naturaliste and Bunker Bay diverge from the great circle defining F_2 between Sugarloaf Rock and Cape Naturaliste. This is interpreted as being due to reorientation by an F_3 fold with an axial trace that passes through west Bunker Bay (see Fig. 7)

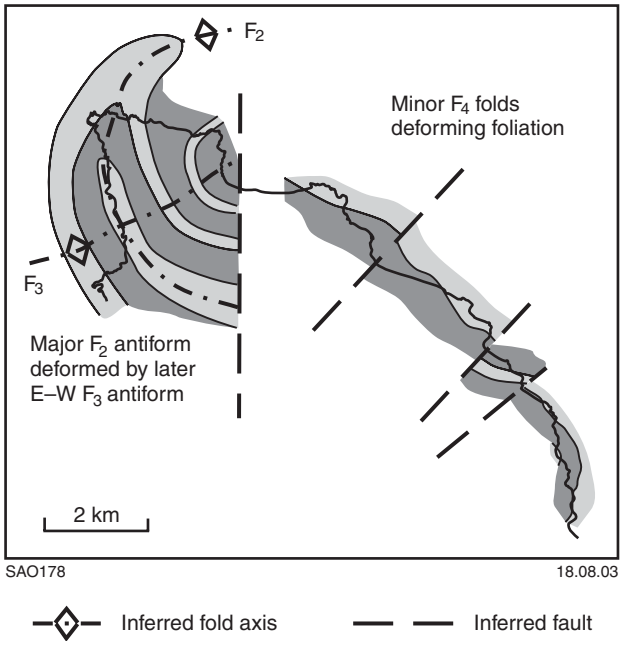

Figure 7. Schematic structural interpretation of the detailed structural map of the northern Leeuwin Complex depicted in Figure 6 (after Collins, in press)

D_1 structures

The dominant D_1 structure is a prominent gneissic foliation in granodiorite and granite gneiss lithologies of the northern Leeuwin Complex, which is folded around the later structures. This foliation is axial planar to local F_1 isoclinal folds defined by lithological boundaries and picked out especially well in metre-scale amphibolite units within the granite gneiss (e.g. at Eagle Bay and Rocky Point). F_1 folds are rootless and where best preserved have no resolvable sense of asymmetry. No consistent D_1 asymmetrical kinematic indicators have been recorded, suggesting that D_1 strain was dominated by pure-shear flattening. Mineral lineations and mineral aggregate lineations are parallel to the hinges of F_1 folds, but increase in intensity westward along the northeast-facing coast towards the core of the F_2 Naturaliste Antiform (see **D_2 structures**), suggesting that the mineral lineation is a composite D_1/D_2 feature.

D_2 structures

The second deformation was responsible for a series of north-trending F_2 folds developed on a range of scales, including the Naturaliste Antiform — a 10 km-scale, north-plunging antiform with its east-dipping axial surface outcropping on the north-facing coast about 500 m east of Cape Naturaliste. The Naturaliste Antiform and associated parasitic folds developed preferentially on its steeper western limb (including the Sugarloaf Antiform; see **Locality 13: Sugarloaf Rock**) are tight asymmetric overturned structures with both the steep, long limbs and shallow, short limbs dipping to the east. Parasitic folds are rare on the shallow-dipping limbs, suggesting that these limbs were under finite extension whereas the steep-dipping limbs were in the finite contraction field. Hinges plunge gently to moderately north-northwest to northeast, parallel to a composite D_1/D_2 mineral lineation. D_2 strain preserved in the northern Leeuwin Complex was dominated by pure-shear east–west shortening, and appears to have been coaxial with D_1 strain, in turn suggesting that D_1 and D_2 structures formed during a single progressive deformation event. The results of this major folding event are well illustrated in a stereographic plot of poles to foliation (Fig. 6).

D_3 structures

S_1 foliations between Cape Naturaliste and Bunker Bay have a different orientation to those from elsewhere, causing the poles to foliation in this region to be deflected away from the D_2 great circle on a stereonet (Fig. 6). Mineral lineations on these foliation planes have also been rotated by the same degree anticlockwise. These deflections can be explained by rotation of the shallow limb of the major F_2 antiform about an east-northeasterly trending F_3 fold that is also responsible for the bend observed in the axial trace of the Naturaliste Antiform and in the lithological boundaries along the west-facing coast near Gull Rock (Figs 6 and 7). No foliations or lineations have been attributed to this folding, which is interpreted as a relatively late north-northwest–south-southeast contractional deformation phase.

D_4 structures

Open undulatory folding of the S_1 foliation along the northeast-facing coast between Dunsborough and Bunker Bay is attributed to a late northwest–southeast contractional phase (Fig. 7). Relative timing relationships between this event and D_2 and D_3 have not been seen.

D_5 structures

An episode of late brittle faulting is inferred from the incised linear gullies present along the northeast-facing coast (Figs 6 and 7). A major north-striking fault may also pass through Bunker Bay, which would explain the different structures seen on either side of this area of no exposure.

Southern Leeuwin Complex

The south-facing coastline between Cosy Corner and Augusta provides an extensive east–west section across the predominantly north-striking structures of the southern Leeuwin Complex (see **Southern Leeuwin Complex** under **Excursion localities**). Although there are some differences between the structural histories of the northern and southern Leeuwin Complex, there is sufficient correlation to suggest that they have both experienced the same deformation events.

D_1 structures

The dominant D_1 structure seen in the field is a gneissic foliation, which is axial planar to F_1 isoclinal folds throughout the area. The isoclines fold earlier lithological layering, and are north-trending, upright to inclined folds, with a gentle plunge and axial planes that dip steeply to

the east. The upright nature of the folds means that fold hinges are rarely spotted on pavement outcrops and are best seen on vertical east–west oriented outcrop surfaces. They can also be identified from repeated lithologies on either side of inferred hinges. An associated mineral lineation, commonly defined by hornblende or biotite, is subhorizontal, except where steepened due to the effects of D_3 (see **D_3 structures** below), and is parallel to the F_1 fold hinges. The scarcity of reliable kinematic indicators and the nature of the folding suggest that D_1 was the result of pure-shear east–west shortening.

D_2 structures

The second deformation produced F_2 folds that are tight to isoclinal in nature and deform the S_1 gneissic fabric. They are coaxial to the folds developed in D_1, suggesting that D_2 is a continuation of the initial D_1 event. Tight F_2 folds are best observed at localities such as Skippy Rock and Elephant Rock, where their exposure is enhanced by a steep northerly plunge. This variation in D_2 orientation is probably due to the effects of D_3 (see **D_3 structures**). D_2 structures in the south seem likely to correlate with D_2 structures described from the northern Leeuwin Complex, although they have a tighter fold style.

D_3 structures

The third deformation to affect the southern Leeuwin Complex produced a west-northwesterly trending regional open warping, with a wavelength of about 10 km. It is identified in the field through an undulation of the L_1 mineral lineation, which varies in orientation from a gentle northerly plunge to a gentle southerly plunge. This variation is seen clearly in stereographic plots of the southern Leeuwin Complex (see **Southern Leeuwin Complex** under **Excursion localities**), which also show that the F_3 folds plunge gently to the west-northwest, rotating the lineations east of their usual north-trending orientation. This deformation has also caused poles to the S_1 foliation to deviate away from a simple D_2 great circle.

D_4 structures

There is little evidence for post-D_3 deformation in the southern Leeuwin Complex, although near-vertical east-trending brittle faults offset earlier structures on a centimetre scale.

Central Leeuwin Complex

Structures in the central Leeuwin Complex have been less well studied than those in the north and south, although preliminary work indicates that most outcrops between Cape Clairault and Cape Freycinet are dominated by high-strain zones of flat-lying foliation, separating lower strain regions characterized by asymmetric folds. Pervasive lineations in the high-strain zones are parallel to fold hinges in the low-strain strains. Their orientation varies from gently northeast plunging to gently southeast plunging, but is consistent at any one outcrop. The relationship between these flat-lying structures and the upright folding identified both to the north and south is unclear at present and the subject of ongoing work.

Low-grade schist

Low-grade metasedimentary rocks of inferred Proterozoic age outcrop at several localities adjacent to the Darling Fault (Fig. 2). The Cardup, Moora, and Badgeradda Groups and Nilling Formation lie to the east of the fault and unconformably overlie the Yilgarn Craton, whereas the Yandanooka Group lies to the west and unconformably overlies the Mullingarra Complex (Myers, 1990a).

The Cardup Group outcrops immediately southeast of Perth (Playford et al., 1976; Wilde and Low, 1980), and comprises folded shale, sandstone, and conglomerate with a pervasive cleavage, and is cut by dolerite dykes. The Moora Group outcrops as a 180 km-long strip between the towns of Moora and Morawa, about 150–300 km north of Perth (Logan and Chase, 1961; Playford et al., 1976; Carter and Lipple, 1982; Baxter and Lipple, 1985). The northernmost outcrops are less than 20 km east of the Mullingarra Complex. The Moora Group has been subdivided into the Billeringa Subgroup — a gently folded series of sandstone, siltstone, basalt, and tuff with a moderate cleavage — and the overlying undeformed sandstone, shale, and dolomite of the Coomberdale Subgroup. Both subgroups are cut by dolerite dykes. The age of the volcanic rocks in the Billeringa Subgroup is poorly constrained by a 1390 ± 140 Ma Rb–Sr isochron (Compston and Arriens, 1968; Giddings, 1976). The Badgeradda Group outcrops about 550 km north of Perth, and comprises folded sandstone, shale, and conglomerate without a penetrative cleavage, whereas the adjacent Nilling Formation (Perry and Dickins, 1960; Baxter, 1974; Low, 1975; Hocking et al., 1982) is composed of folded greywacke and sandstone with a spaced cleavage. The Yandanooka Group (Playford et al., 1976; Baxter and Lipple, 1985) comprises undeformed but steeply dipping siltstone, conglomerate, and sandstone, and lies adjacent to the Moora Group, but on the opposite side of the Darling Fault. It is not cut by mafic dykes, and is likely to be younger than the nearby Billeringa Subgroup given that the metamorphic age of the underlying Mullingarra Complex gneiss is younger than the Rb–Sr age for the volcanic components of the Billeringa Subgroup.

Little else is known about these units, although they are thought to have been deposited during the late Mesoproterozoic to Neoproterozoic. The degree of deformation and dip of the bedding commonly increases towards the Darling Fault, suggesting that deformation may be related to movements along the Proterozoic precursor to this structure. Variable relationships reported for these units with respect to deformation and dyke emplacement suggest that geochronological studies of detrital and metamorphic minerals in these rocks could provide valuable constraints on the evolution of the Pinjarra Orogen.

Darling Fault Zone

There is widespread field and isotopic evidence for reworking of the westernmost Yilgarn Craton and Albany–

Fraser Orogen during the development of the Pinjarra Orogen. The most obvious features are three swarms of subvertical dolerite dykes assumed to have intruded in the late Mesoproterozoic to Neoproterozoic (Fig. 4a; Myers, 1990a). The 755 Ma Mundine Well dyke swarm cuts the Yilgarn Craton and Northampton Complex, as well as the Gascoyne Complex and Pilbara Craton to the north (Wingate and Giddings, 2000), and its northeasterly trend is consistent with dextral movement along the Pinjarra Orogen at this time (as discussed in **Northampton and Mullingarra Complexes**). The Muggamurra dyke swarm cuts the northwestern Yilgarn Craton and Moora Group, and changes trend from northeasterly to east-northeasterly away from the Darling Fault. Recent isotopic studies have identified at least two different dyke generations in this swarm, with crystallization ages of about 1200 and 1070 Ma (Wingate, M. T. D., 2003, written comm.). The Boyagin dyke swarm cuts across much of the southwest, including the Yilgarn Craton, Albany–Fraser Orogen, Moora Group, and Cardup Group (Prider, 1948; Myers, 1990a; Harris and Li, 1995) and the trend changes from north-northwesterly to northwesterly away from the Darling Fault, subparallel to a set of faults that cut the southwest Yilgarn Craton. Dyke orientation is consistent with sinistral movement along the southern Pinjarra Orogen at the time of emplacement, which is believed to be 550–500 Ma from palaeomagnetic constraints (Harris and Li, 1995) and 590–560 Ma from Rb–Sr dating of the sheared margins of a dyke (Compston and Arriens, 1968).

Structural reworking of the Darling Fault Zone is dominated by a regional-scale sinistral rotation of originally west-striking structures in the westernmost Albany–Fraser Orogen through 90° (Fig. 2) to bring them parallel to the Pinjarra Orogen (Beeson et al., 1995). At outcrop scale, north-trending amphibolite-facies mylonite zones are common within 20 km of the Darling Fault along the western edge of the Albany–Fraser Orogen (Beeson et al., 1995) and Yilgarn Craton (Lister and Price, 1978; Blight et al., 1981; Bretan, 1986). These mylonites are best studied in the region between the Moora Group and Albany–Fraser Orogen, where they show evidence for at least three stages of movement (Bretan, 1986). Steep dip-slip lineations probably reflect Phanerozoic reactivation of these structures during Gondwana breakup, but earlier subhorizontal lineations record a Precambrian strike-slip history, consistent with geophysical evidence that the present-day Darling Fault has reactivated an older subvertical transcurrent fault that penetrates the entire crust (Dentith et al., 1993). Kinematic data predominantly indicate sinistral strike-slip movement, consistent with the observed sense of drag on the Albany Belt, but there is also limited microstructural evidence for an earlier stage of dextral wrenching (Bretan, 1986). The age of any dextral motion is poorly constrained. Blight et al. (1981) reported late Archaean 2575 Ma Rb–Sr whole-rock ages for the Logue Brook Granite near Harvey, and retrieved identical ages for samples of undeformed granite and highly deformed granite within a north-trending mylonite of the Darling Fault Zone. They interpreted these data as evidence for Archaean deformation immediately after granite crystallization, leading Bretan (1986) to suggest that the dextral stage of movement was also late Archaean. However, Blight et al. (1981) acknowledged that the Rb–Sr system might not have been reset on a whole-rock scale during mylonite deformation, in which case deformation could be significantly younger than Archaean. Fitzsimons (2001, 2003) suggested that this dextral movement could have been synchronous with 750 Ma dextral wrenching in the Northampton Complex.

Further constraints on the timing and nature of dextral and sinistral wrenching are provided by Rb–Sr biotite ages (Fig. 4b; de Laeter and Libby, 1993; Libby and de Laeter, 1998; Libby et al., 1999), which decrease systematically westward across the Yilgarn Craton and Albany–Fraser Orogen, defining the Eastern, Transitional, and Western Biotite Zones of Libby and de Laeter (1998). This pattern of decreasing ages changes markedly from north to south along the Darling Fault Zone. A broad region of 2000–1500 Ma biotite ages in the northwestern Yilgarn Craton probably reflects the Capricorn Orogeny, but only a narrow zone of resetting is apparent near the Mullingarra and Northampton Complexes, and Rb–Sr biotite ages in this part of the craton margin are no younger than 1680 Ma. As noted above, this implies limited local thermal activity during the Mesoproterozoic and Neoproterozoic. In contrast, a broad region of resetting down to 450 Ma in the southwest must reflect a significant late Neoproterozoic to early Palaeozoic thermal event. This is likely to be related to the sinistral transcurrent movement, which caused pervasive deformation and metamorphism in the Leeuwin Complex and the southwestern margins of the Yilgarn Craton and Albany–Fraser Orogen. The lack of penetrative sinistral wrenching at 550 Ma in the Northampton and Mullingarra Complexes indicates that this later phase of deformation was focused west of these two terranes (Harris, 1994a), which remained attached to the Yilgarn Craton, whereas the Leeuwin Complex was probably translated southward to its present position at 550–500 Ma.

It is of note that the sinistral accretion of the Leeuwin Complex at 550–500 Ma had a much greater thermal and structural impact on the cratonic margin of Western Australia than the inferred dextral accretion of the Northampton and Mullingarra Complexes at about 750 Ma. Palaeomagnetic and geological evidence from India, Antarctica, and Australia indicates that India and Australia amalgamated at about 550 Ma along a wide zone of deformation and metamorphism (Powell and Pisarevsky, 2002; Fitzsimons, 2003; Pisarevsky et al., 2003). The Pinjarra Orogen in Western Australia represents the eastern margin of this suture zone, suggesting that sinistral strike-slip along the Darling Fault Zone at this time was the result of a major oblique collision between India and Australia. Upright north-trending folds in the northern and southern Leeuwin Complex most likely developed during this event (Collins, in press), and indicate that some internal components of the orogen underwent east–west shortening at the same time as north–south transcurrent movement along the edge of the orogen. The lack of a pervasive thermal or structural overprint at 750 Ma suggests that any terrane movement at this time was associated with transcurrent transport, but not with a significant collision event.

Basement to the Perth Basin

Fletcher et al. (1985) and Fletcher and Libby (1993) reported isotopic data for samples recovered from five drillcores through the Perth Basin that intersected crystalline basement at depths ranging from 200 to 3055 m. Samples of garnet-bearing gneissic granite and coarse- to medium-grained granite from the northern Perth Basin, west of the Mullingarra Complex, yielded T_{DM} Nd model ages of 2200–2000 Ma, whereas samples of granite gneiss, garnet–biotite meta-syenogranite, and garnet–biotite monzosyenite gneiss from the southern Pinjarra Orogen, immediately east of the Leeuwin Complex, yielded T_{DM} Nd model ages of about 2000 Ma. These ages correspond closely to 2100–2000 Ma T_{DM} Nd model ages obtained from the exposed Northampton and Mullingarra Complexes (Fletcher et al. 1985), but are significantly older than ages retrieved from the Leeuwin Complex. These data suggest that the Leeuwin Complex contains younger protoliths than Proterozoic rocks to the immediate east, and confirm that the Pinjarra Orogen comprises terranes of markedly different age close together (Fletcher and Libby, 1993), which is consistent with the models of strike-slip movement and terrane accretion outlined above.

Excursion localities

The descriptions below include directions on how to get to each location. These directions are given as a continuous route from one locality to the next, even though the sites listed are designed to fill a three-and-a-half day field excursion. In practice the route will vary because of the need to return to accommodation each evening.

Darling Fault Zone

Locality 1: Harvey Weir Spillway

Travel south from Perth along the South Western Highway, and turn left at the Harvey junction onto Weir Road (about 140 km south of Perth). Follow Weir Road for 2.4 km, and then turn left into the tourist area at the dam wall. Go down to the bottom car park, follow the path down past the grass and walk across the footbridge, passing over some rounded mylonite outcrops to the left. Turn towards the wire fence to the west, and walk around the southern end to gain access to the spillway. Permission should be obtained from the Water Corporation before entering the spillway.

The blasted walls of the spillway provide an excellent opportunity to view a typical mylonite of the Darling Fault Zone within the porphyritic upper Archaean Logue Brook Granite (Blight et al., 1981). A foliation dips steeply to the west and an intense lineation defined by stretched feldspar porphyroclasts and elongate mineral aggregates plunges shallowly to the north, consistent with transcurrent movement along the north-trending Darling Fault Zone. There are few unambiguous kinematic indicators to give the sense of strike-slip at this locality, although some of the feldspar porphyroclasts appear to show a consistent sense of obliquity to the dominant lineation. Mafic dykes have been deformed within the mylonite zone and injected by pegmatitic melt veins. This locality is close to where Blight et al. (1981) collected their samples of mylonite for Rb–Sr geochronology, which yielded an isochron that was indistinguishable in age from their 2577 ± 50 Ma isochron for undeformed Logue Brook Granite. This late Archaean emplacement age has been confirmed by SHRIMP U–Pb zircon analyses of a mylonite sample from Harvey Dam (Nelson, in prep.), which yielded a concordant zircon population at 2607 ± 3 Ma, interpreted as the age of igneous crystallization. A complex discordance pattern indicates episodes of both ancient and recent lead loss (Nelson, in prep.), but does not provide conclusive evidence of the timing of deformation.

Locality 2: Roelands Granite Quarry

Continue south along the South Western Highway from Harvey for about 23 km to the Roelands turn-off. Turn left and follow Government Road towards Roelands, cross the railway, follow the right bend in the road, and then take a left turn 200 m from the Highway onto Waterloo Road. Here there is a bitumen road to the left and a gravel road to the right. Take the gravel road and follow it, with the fenceline on your left, for 1.2 km, where there is a narrow cutting. Take the track to the right of the cutting and continue for another 1.2 km to a fork in the road. Take the right-hand fork and continue for 300 m to the outcrops on the left-hand side of the track, which are just a few hundred metres before the entrance to the disused quarry. Permission to visit these outcrops should be obtained from the Department for Planning and Infrastructure (Bunbury Office).

This quarry provided granite blocks for Bunbury Harbour, and the outcrops display another example of a Darling Fault Zone mylonite developed in the porphyritic Logue Brook Granite (Fig. 8). It displays a greater strain variation than the rocks at Harvey, but still has a shallow, northerly plunging lineation, and in this case the feldspar grains form sigma clasts indicative of a sinistral strike-slip sense of movement. Evidence for sinistral strike-slip is common in Darling Fault Zone mylonites of the southwest Yilgarn Craton and Albany–Fraser Orogen (Bretan, 1986; Harris, 1994a; Beeson et al., 1995), and probably reflects the accretion of the Leeuwin Complex to the Australian craton at 550–500 Ma.

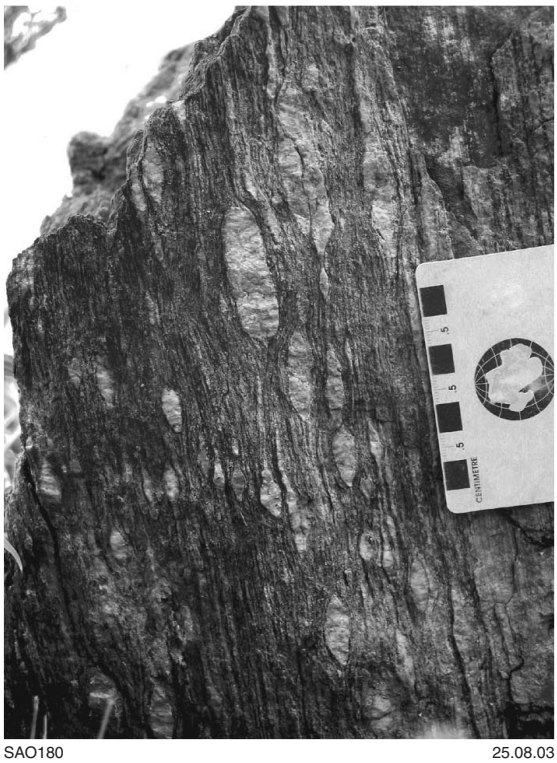

SAO180 25.08.03

Figure 8. Augen mylonite at Roelands Granite Quarry. This is the underside of a face that dips north into the outcrop, and has a subvertical foliation and subhorizontal lineation consistent with transcurrent movements along the Darling Fault Zone. Some of the feldspar augen in the field of view have sigma-clast morphologies indicative of dextral movement, which actually corresponds to sinistral movement when viewed from above

Southern Leeuwin Complex

Locality 3a: Skippy Rock (north)

From Roelands take the South Western and Bussell highways south via Bunbury and Busselton to Augusta (about 150 km in total). Continue south from Augusta along Leeuwin Road towards Cape Leeuwin (Fig. 9). Ignore the first right turn onto the Skippy Rock Road circuit, about 4 km from the Augusta town centre, and instead follow the bend in the Leeuwin Road to the right, and take the next right turn onto the other end of Skippy Rock Road, which is about 7 km from Augusta. Follow this 2WD gravel road and take the second turn on the left, which is about 1 km from the Leeuwin Road junction, and continue for another 1 km to the car park at the end of the road. Take the narrow path that leads down to the sea from the northern end of the car park. At the end of the path continue westward for about 200 m along the black ilmenite- and garnet-rich mineral sands to the outcrops at the end of the small peninsula.

There are a number of lithologies at this locality including amphibolite, garnet-rich migmatite gneiss, and felsic gneiss with minor garnet. All lithologies have been folded into isoclinal structures, with axial planes that dip steeply to the east and hinges that plunge gently to moderately to the north. A synform cored by amphibolite and exposed halfway along the northern edge of the outcrop is one of the best examples of an F_2 fold (Fig. 10), which clearly deforms the earlier S_1 gneissic foliation. Most lithologies show evidence of partial melting. Abundant leucosomes contain mafic minerals, the identity of which depends on the host-rock chemistry, indicating a local control on melt composition. Leucosomes are particularly well developed in the garnet-rich migmatite, which is one of the few lithologies in the Leeuwin Complex that lacks definitive evidence of an igneous origin and might have had a sedimentary precursor, although this is difficult to prove. Garnet is concentrated in centimetre-scale ovoid leucosome patches and veins, which are depleted in biotite compared with the host rock, indicating that biotite and garnet were a reactant and product, respectively, of the partial melting reaction. Biotite selvages are particularly well developed around the larger segregations and veins, suggesting back-reaction of the partial melt with the host rock on crystallization.

Leucosomes are aligned parallel to the dominant foliation and lineation in the outcrop, but they appear internally undeformed and have a granoblastic texture. This suggests that partial melting was synchronous with the last pervasive deformation in the rock, but that the melt crystallized at least in part after that deformation. The larger veins are locally deformed into ptygmatic folds, and the foliation of the host rock is axial planar to these folds. It is unclear whether these folded leucosomes were deformed in D_1 or D_2, but they were synchronous with peak metamorphism. Zircons have been separated from a sample of the garnet-rich migmatite, and a preliminary assessment of unprocessed U–Pb SHRIMP analyses of these grains reveals an age of 800–500 Ma for grain cores and an age range of 700 to 500 Ma for rims. Given that partial melting appears to have been the last pervasive recrystallization event in this rock, and that this is likely to have been accompanied by new zircon growth, these data constrain peak metamorphism and melting at Skippy Rock to 550–500 Ma. An interpretation of the older cores and rims must await full processing of the data.

Locality 3b: Skippy Rock (south)

Return to the car park and take the steps down to the outcrops immediately below. Turn left and walk southward along the coastal exposure for about 100 m to a flat wave-cut platform.

The dominant lithologies at this locality are steeply dipping, north-trending amphibolite and granite orthogneiss, and they were mapped in detail by Myers (1994; Fig. 11). Intense deformation has destroyed any evidence of primary contact relations, and both the amphibolite and granite orthogneiss are probably composite lithologies. Myers (1994) suggested that the amphibolite was derived by deformation of gabbro and leucogabbro precursors, whereas the granite gneiss contains discontinuous pegmatite layers, and was probably derived by repeated deformation of locally derived pegmatite vein networks in a relatively even-grained granite. Folds are visible on all scales at this outcrop. Myers (1994) interpreted the complex outcrop patterns as reflecting refolded isoclinal folds, and it is likely that the two major amphibolite layers exposed on this platform are actually a single layer deformed into a 100 m-scale isoclinal fold that closes to the south. Structures are particularly complex close to the boundaries between amphibolite and granite gneiss (Fig. 12), with centimetre-scale parasitic folds and oblique pegmatite veins in the amphibolite that appear to flare out towards the contacts. In the centre of the amphibolite units the same veins are parallel to the north-trending foliation.

Locality 4: Cape Leeuwin lighthouse

Return to the car park, drive back to Skippy Rock Road, turn right, continue back to Leeuwin Road, and then turn right and drive for about 1 km to the lighthouse. Park at the lighthouse car park in front of the gates, and walk a few tens of metres down the slope east of the car park to the outcrop.

Cape Leeuwin consists of felsic gneiss derived by intense deformation of a granite. The gneiss contains quartz, alkali and plagioclase feldspar, hornblende, and biotite. It contains thin layers of pegmatite and granite that have been strongly deformed and attenuated along with the host rock, and now lie subparallel to the main north-trending foliation of the gneiss. Evidence of north–south extension is provided by local boudinage of the gneissic foliation, with pegmatite patches in boudin necks indicating migration of partial melt into relatively low-pressure regions of the rock (Fig. 13).

Nelson (1996) dated a sample of this same hornblende granite gneiss, collected just south of the lighthouse. SHRIMP U–Pb analyses of zircons from this sample yielded a single age population of 681 ± 10 Ma, interpreted as the time of protolith granite crystallization.

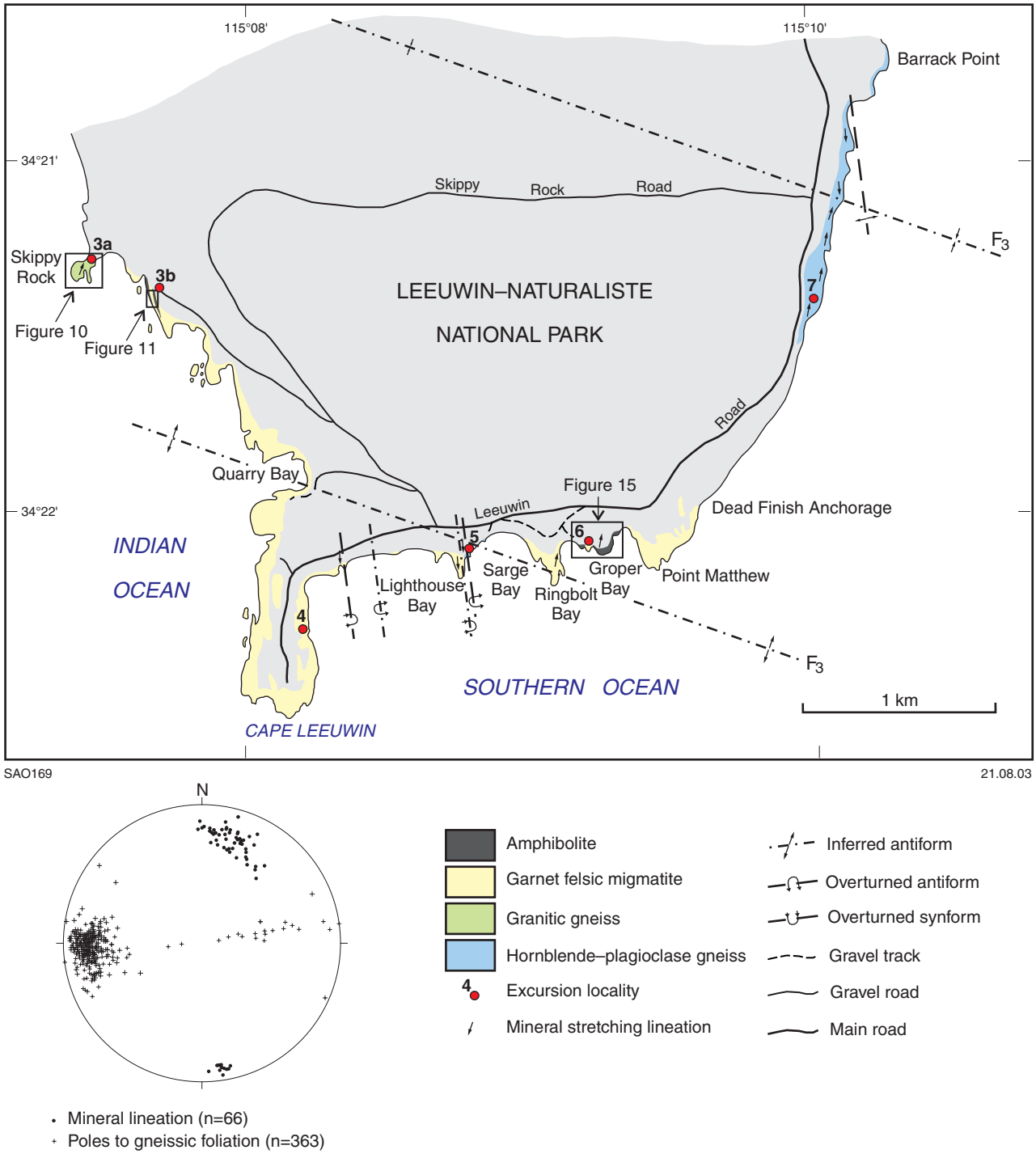

Figure 9. Map of the southern Leeuwin Complex from Skippy Rock to Barrack Point. The positions of Localities 3 to 7 are shown, as are the locations of detailed outcrop maps. Also shown are the fold axes associated with various deformation events. The stereonet (lower hemisphere, equal-area projection) shows the general north trend of the structures, and the deviation of the gently plunging stretching lineation due to the effects of F_3

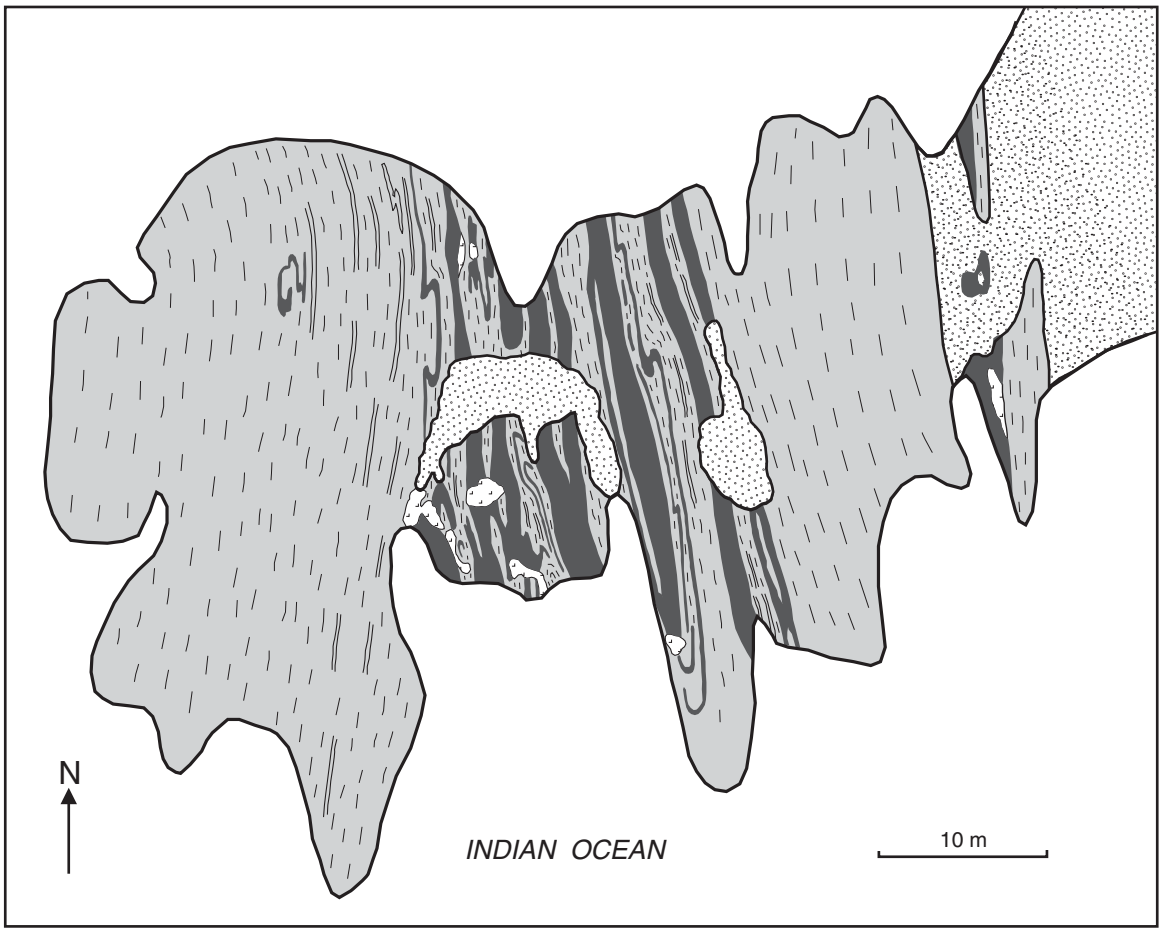

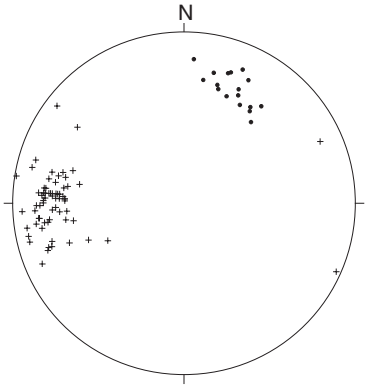

• Mineral lineation (n=17)
+ Poles to gneissic foliation (n=67)

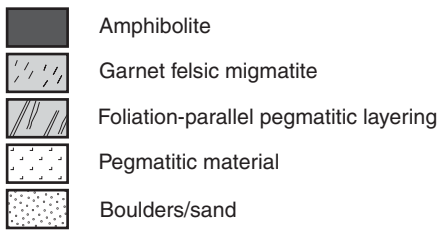

Figure 10. Detailed outcrop map of Skippy Rock (Locality 3a) showing the D_1/D_2 isoclinal folding of interleaved mafic bands and garnet-bearing felsic migmatite. The foliation and lineation observed here are similar in orientation to those throughout the southern Leeuwin Complex, although minor variations on a local scale are attributed to a D_3 folding event

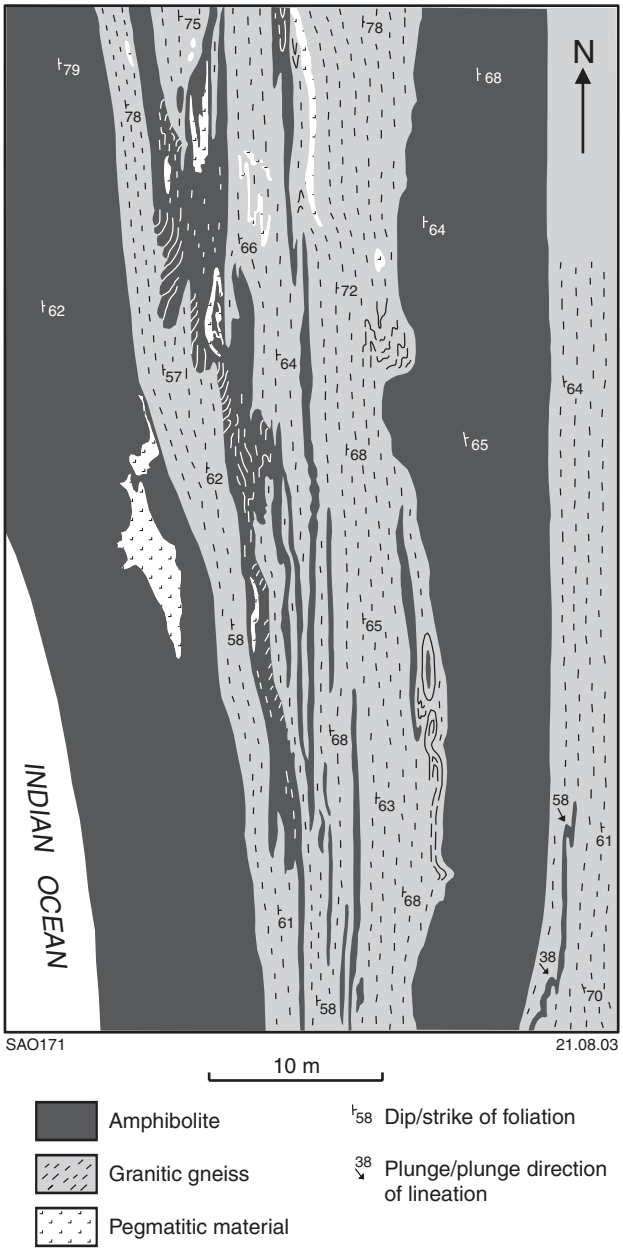

Figure 11. Detailed map of the rock pavement southwest of Skippy Rock car park (Locality 3b), displaying intensely deformed and interlayered amphibolite and pegmatite-banded granite gneiss (after Myers, 1994)

Figure 12. Interlayered amphibolite and granite gneiss southwest of Skippy Rock car park (Locality 3b), showing folding of the steeply dipping lithological boundary and the change in orientation of pegmatite veins close to that boundary. Photograph taken looking south

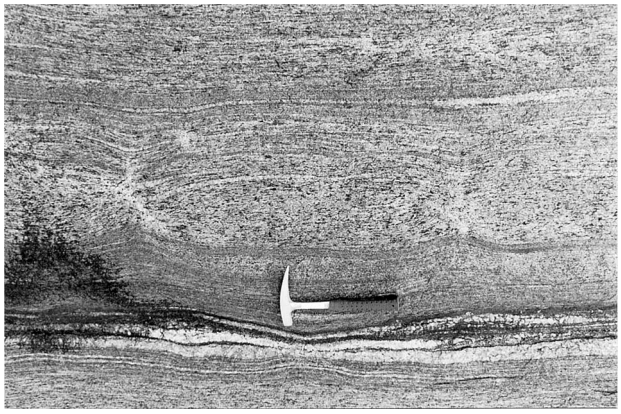

Figure 13. Pavement outcrop northeast of Cape Leeuwin lighthouse (Locality 4) displaying boudinage of the pervasive steeply dipping S_1 foliation. Pegmatite has migrated to the boudin necks. North is to the right of the photograph

Locality 5: Sarge Bay

Drive back along Leeuwin Road from the lighthouse, and about 300 m after the Skippy Rock Road turn-off take a right turn off Leeuwin Road onto an unmarked 2WD gravel track (1.3 km from the lighthouse). Follow this short track to the car park at the end, and walk west along the beach for about 100 m to the first main outcrop.

The first major outcrop encountered on the beach is a garnet-bearing hornblende–plagioclase gneiss, which displays a pervasive mineral-stretching lineation that plunges gently to the south (Fig. 14). This outcrop is interpreted as the hinge zone of an isoclinal F_1 fold, where local constrictional strain has caused the lineation to dominate over planar fabrics. This lithology was considered by Myers (1990b) to be part of the dismembered and transposed Augusta Anorthosite Complex (see **Locality 7**).

Farther west along the beach towards the headland is a homogenous hornblende-bearing granite gneiss, which displays a steeply dipping, north-trending foliation and contains a well-exposed boudinaged mafic layer, indicating north–south extension. The concentration of pegmatite at boudin necks indicates melt migration during deformation, and suggests that peak metamorphism was more or less synchronous with this deformation. This outcrop is along strike from similar granite gneiss exposed at the junction between Leeuwin and Skippy Rock roads,

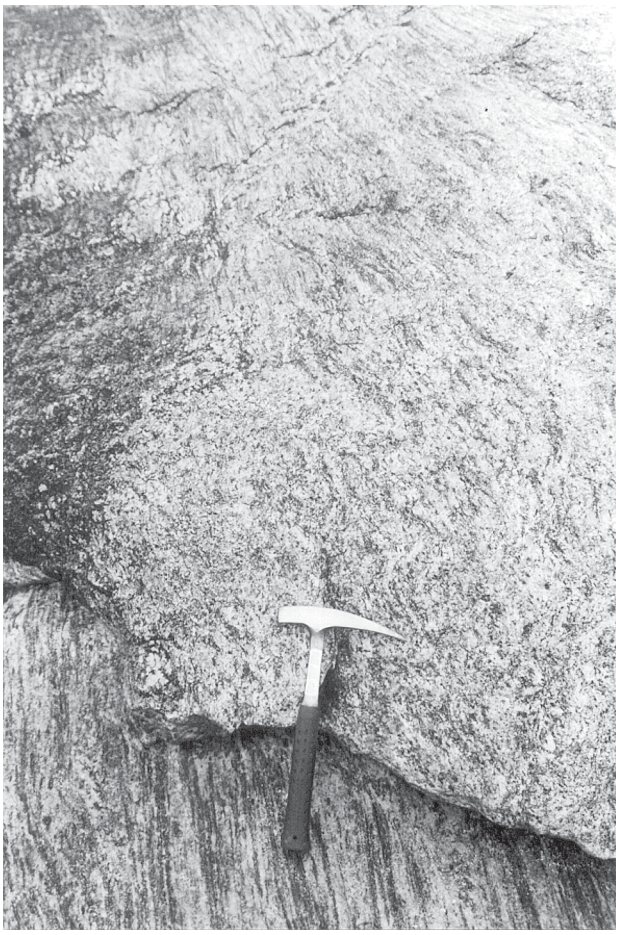

SAO183 18.08.03

Figure 14. Outcrop of garnet-bearing hornblende–plagioclase gneiss from the hinge region of an F_1 fold at Sarge Bay (Locality 5). The intense mineral-stretching lineation plunges shallowly to the south and developed due to the constrictional strain in the fold hinge

which was sampled by Nelson (1996) for geochronology. SHRIMP U–Pb analyses of zircons from the sample at that site yielded a dominant age population at 688 ± 7 Ma, which is identical to the age of the gneiss at Cape Leeuwin lighthouse, and interpreted as an igneous crystallization age. Three zircon grains from the sample provided evidence for isotopic disturbance some time after igneous crystallization, presumably reflecting high-grade metamorphism.

Locality 6: Ringbolt Bay

Return to Leeuwin Road and turn right towards Augusta. Turn onto the second 2WD gravel track on the right, about 500 m after the Sarge Bay turn-off. Follow the track for about 200 m and then turn left off the main track to the car park. Walk east from the car park along the beach for about 20 m to the outcrop. This is the western edge of the mapped area shown in Figure 15.

Outcrops on the eastern side of Ringbolt Bay comprise layers of recrystallized and deformed anorthosite, leucogabbro, and gabbro (now amphibolite) interleaved with pegmatite-banded granite gneiss and a massive amphibolite layer that may be derived from a mafic dyke. Figure 15 is a detailed map of this outcrop, although it has not attempted to distinguish the different varieties of amphibolite. These rocks have been attenuated and boudinaged in a north–south direction, and folded into tight and isoclinal F_1 and F_2 folds. North-trending foliations and fold-axial planes dip steeply to the east, and lineations plunge gently to the north at this locality. Fluctuations in the lineation plunge direction along this south-facing coast are thought to reflect open, northwest-trending upright D_3 folds.

Locality 7: Northeast of Point Matthew

Return to Leeuwin Road and turn right towards Augusta. Continue for 2 km, following the left-hand bend in the road, and turn in to one of the gravel parking bays on the right side of the road. Walk east for 10 m to the outcrops.

This outcrop was mapped by Murphy (1992) as hornblende–plagioclase gneiss, and interpreted by Myers (1990b) as part of a layered anorthosite intrusion — the Augusta Anorthosite Complex — deformed and metamorphosed under high-grade conditions. The gneiss consists predominantly of plagioclase and hornblende, together with quartz, alkali feldspar, garnet, ilmenite, zircon, sphene, and allanite (Murphy, 1992). Plagioclase is labradorite to bytownite (An_{60} to An_{74}) in composition. The rocks here display a well-defined foliation that dips moderately to the west. Between this locality and Barrack Point, farther along the coast to the northeast, this foliation swings around a regional F_2 antiform and becomes easterly dipping. A lineation is developed locally, and plunges gently to the north or south. Changes in the orientation of D_1 and D_2 structures along this north–south section of coastline define the location of F_3 hinge zones (Fig. 9).

Myers (1990b) identified a number of lithologies that he considered part of the Augusta Anorthite Complex, including garnet anorthosite (as seen at Locality 5), layered anorthosite comprising anorthosite, leucogabbro, and gabbro (now metamorphosed to amphibolite), and mottled anorthosite. The latter contains relict orthopyroxene oikocrysts, now deformed into ovoid aggregates of metamorphic orthopyroxene, hornblende, and biotite. Nelson (1995) stated that a sample of anorthosite collected a few hundred metres north of this locality contained insufficient zircon to date, although an unpublished U–Pb SHRIMP zircon age of about 700 Ma for a hornblende meta-anorthosite from the Leeuwin Complex was obtained by M. T. McCulloch (reported by Black et al., 1992).

Locality 8a: Cosy Corner

Return to Augusta, and continue northward along the Bussell Highway for 3 km and turn left onto Caves Road. Continue along Caves Road for 11 km and turn left onto Cosy Corner Road. Follow this 2WD gravel road for about 4 km to the car park at the end (Fig. 16). Localities 8a–c can all be reached on foot from the Cosy Corner car park.

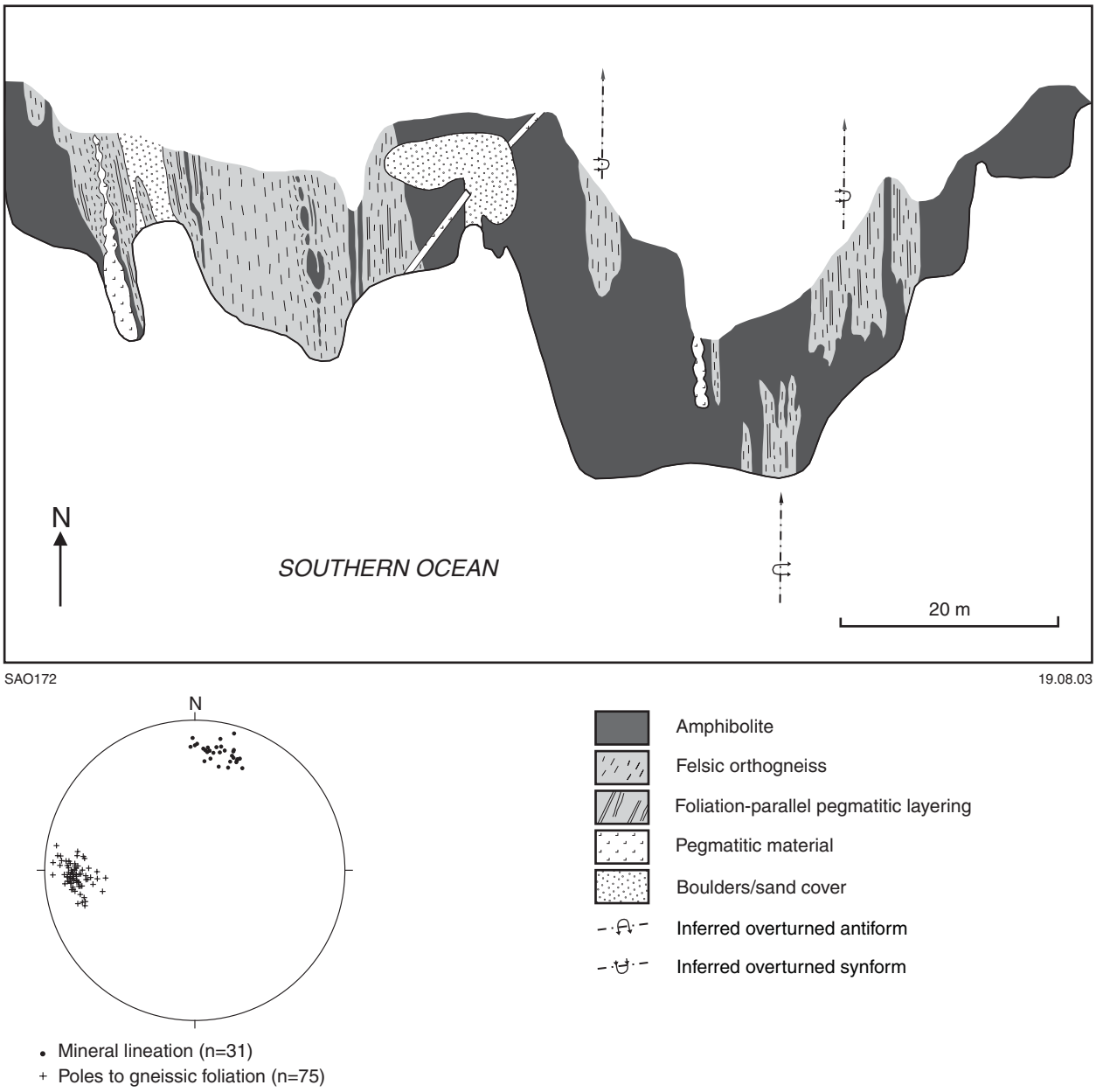

Figure 15. Detailed map of pavement outcrops at Ringbolt Bay (Locality 6), where a large amphibolite band is interleaved with gabbroic to granitic gneisses, and has undergone folding and extension. Structural data shown on the stereonet (lower hemisphere, equal-area projection) display a consistently steep, easterly dipping foliation, with a lineation that plunges gently to the north

An alternative 4WD route is available for Localities 8b and c (Fig. 16). Turn left off Cosy Corner Road onto the Cape-to-Cape Track, about 2.5 km after leaving Caves Road, and follow the track southward, winding up a ridge and then down the other side. About 1.7 km along the track, near the bottom of the ridge, there is a junction. Continue straight on to get to Elephant Rock (Locality 8b) or turn left to continue southward to Deepdene Beach (Locality 8c).

The structure at this locality is best seen on a sloping wave-cut platform at the end of a small headland to the west of the car park (Fig. 17). Lithologies here comprise a garnet-bearing granite gneiss with pegmatitic layering and foliation defined by mafic minerals, a garnet-bearing granite gneiss with no fabric-defining mafic minerals, and a granodiorite gneiss with a weak foliation and a more granoblastic texture. Any original contact relationships have been obliterated, and contacts between these lithologies are diffuse. The foliation trace trends dominantly northeast and appears to be axial planar to a series of tight folds in the lithological layering, best picked out by amphibolite layers, with the hinges plunging shallowly to about 077°.

The cliffs just north of this locality contain a thick amphibolite layer at their base, which appears to be dipping shallowly to the east. A kilometre north of this locality, in Foul Bay, a garnet-rich gneiss with a strong mineral lineation defined by the garnet, plunges shallowly to about 055°.

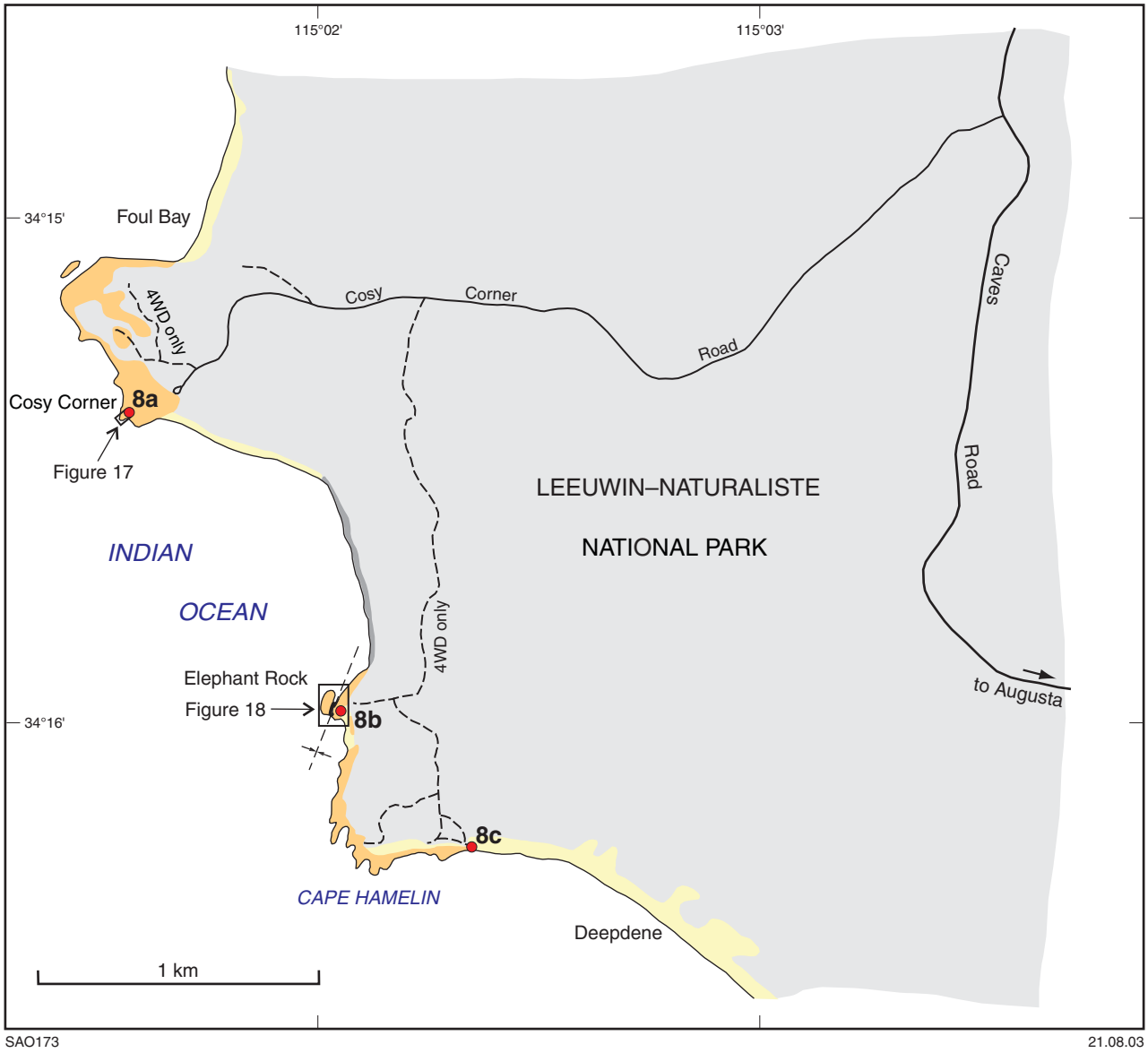

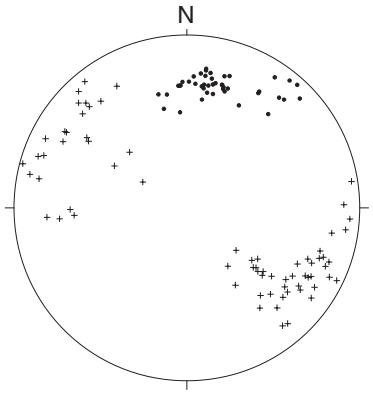

- Mineral lineation (n=44)
+ Poles to gneissic foliation (n=70)

Recent sand
Quaternary limestone
Amphibolite
Felsic orthogneiss

8a Locality number
Synform
Gravel track
(2WD unless indicated otherwise)
Gravel road
Main road

Figure 16. Map of the Cosy Corner area from Foul Bay to Deepdene (Localities 8a,b,c), showing the locality positions, pertinent roads and tracks, and the extent of basement outcrops. Also shown are the areas of more detailed maps presented elsewhere in this field guide and the major structures observed in the field. Structural data plotted on a stereonet (lower hemisphere, equal-area projection) suggest that the major isoclinal folds and associated lineations have been rotated by varying degrees towards the northeast, compared with their northerly trends near Cape Leeuwin. Similarly, the poles to foliation have been deflected away from the simple east–west F_1/F_2 great circle typical of Cape Leeuwin gneisses by the effects of D_3 warping

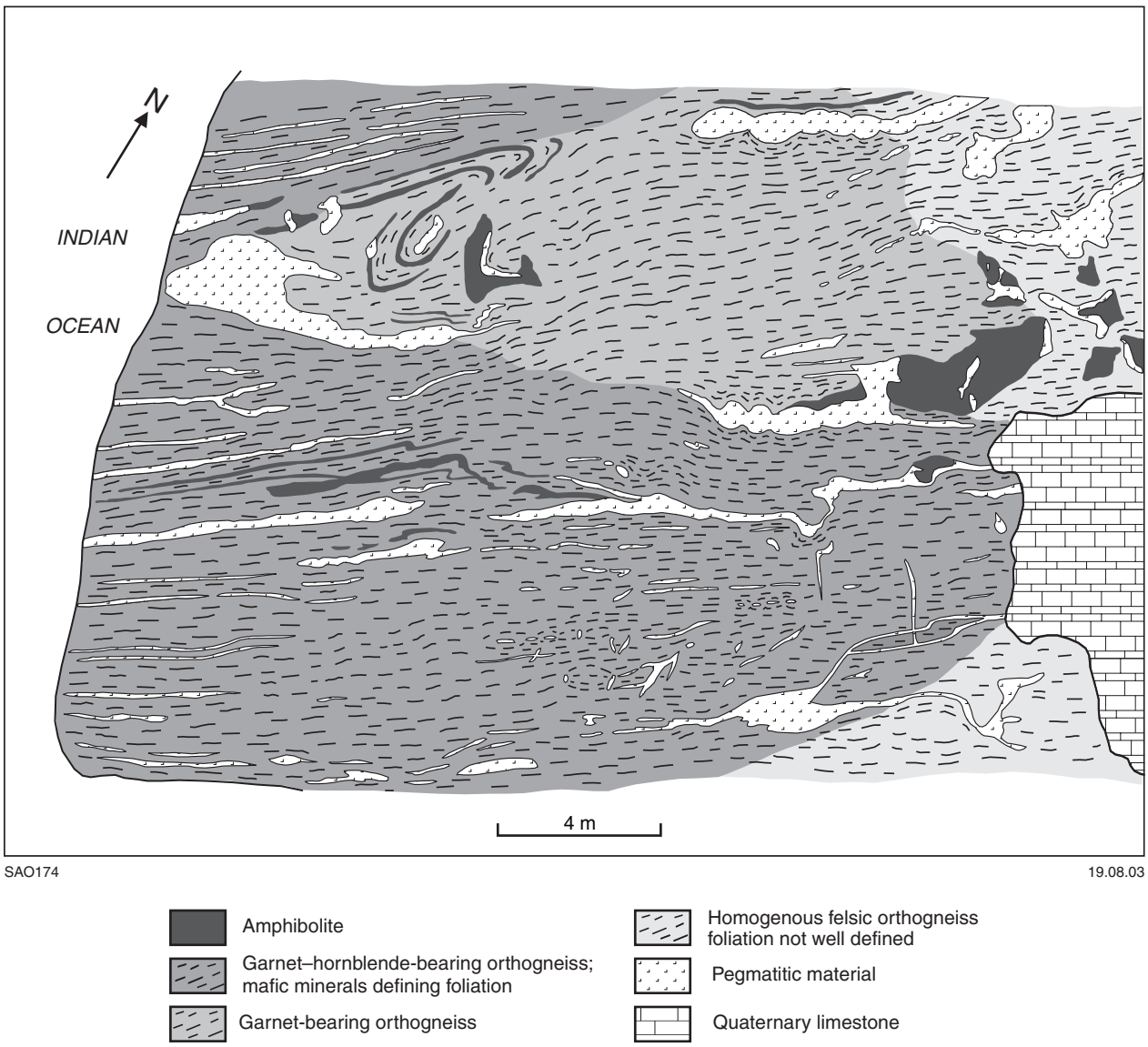

Figure 17. Detailed outcrop map of a wave-cut platform at Cosy Corner (Locality 8a) that displays the blurred contact between garnet–hornblende gneiss and homogenous granodiorite gneiss. There are no sharp contacts, and these lithologies have been flattened and folded, as have associated pegmatite and mafic layers

Granite gneiss immediately west of the Cosy Corner car park is granoblastic with an intense foliation, and a sample of this rock was collected for geochronology by Nelson (1996). SHRIMP U–Pb zircon analysis revealed a dominant age population at 779 ± 23 Ma, interpreted as the time of igneous crystallization of the granite protolith.

Another group of four analyses were interpreted by Nelson (1996) to reflect a metamorphic event at 605 ± 36 Ma associated with nebulous leucosome patches in the rock. However, Collins (in press) questioned the interpretation of this younger age population, noting that the analyses are reverse discordant and intercept the concordia close to 550 Ma, suggesting that the metamorphism and associated isotopic disturbance could have occurred at about 550 Ma rather than at 605 Ma.

Locality 8b: Elephant Rock

Walk east from the car park and take the path down the steps to Cosy Corner Beach below the car park. Walk east along the beach for about 600 m to the narrow limestone platform, and walk along the top of the platform for another 600 m towards the basement rocks, noting the karst features and cylindrical solution holes. Follow the coast for another 200 m towards the rounded elongate grey headland known as Elephant Rock.

This locality comprises felsic gneiss and amphibolite layers, which have been deformed into a gently northerly plunging isoclinal synform (Fig. 18), with an axial plane dipping steeply to the east. Parasitic folds to this major

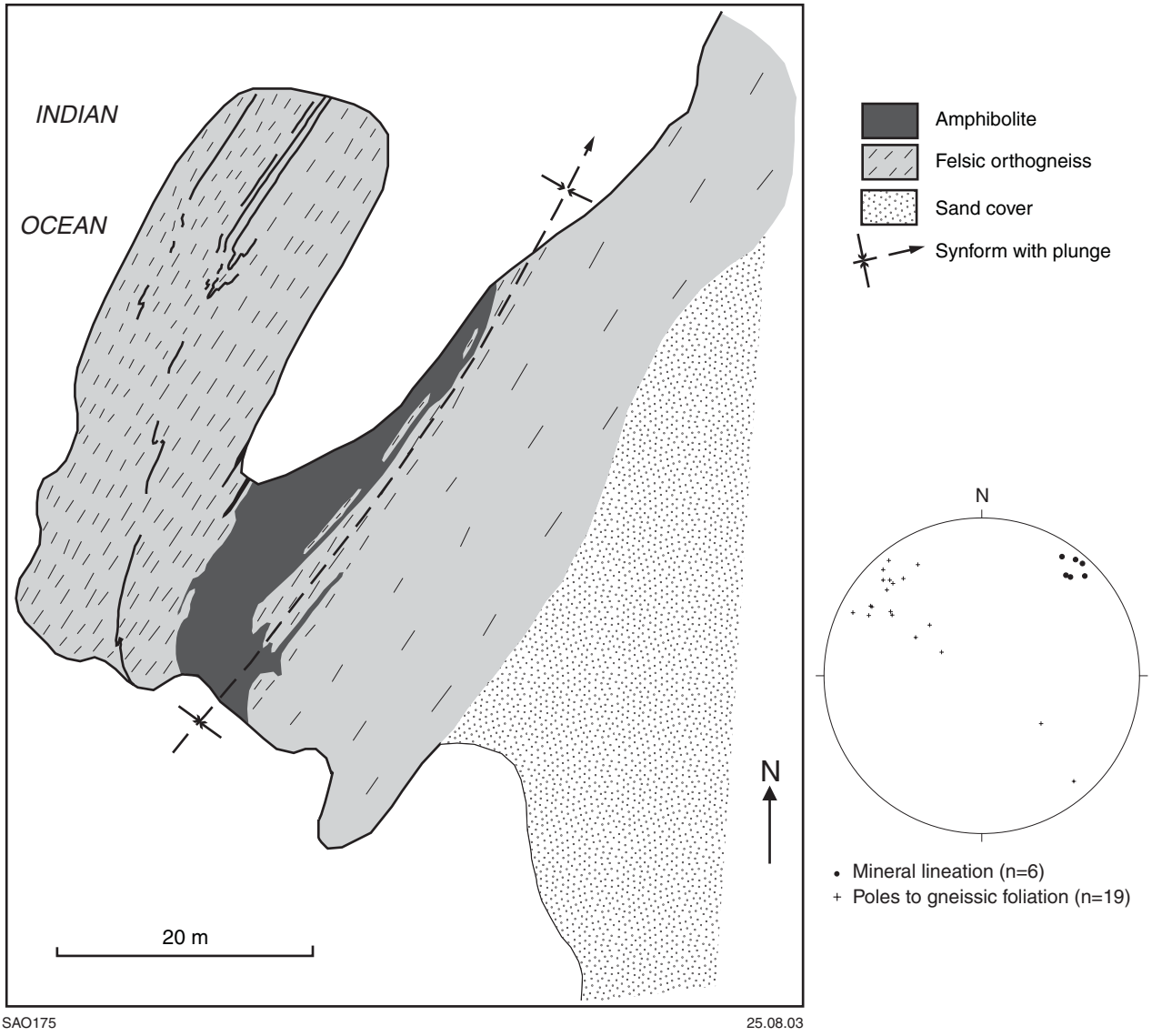

Figure 18. Detailed outcrop map of Elephant Rock (Locality 8b) displaying amphibolite and granite gneiss folded into tight northwest-trending F_1 structures with steep, easterly dipping axial planes and a shallow northeasterly plunge

structure are particularly well exposed on the western limb, and defined by a thin (10 cm) amphibolite layer within the granite gneiss.

The main foliation is axial planar to this folding event (Fig. 19), but has also been affected by extension causing boudinage of the amphibolite layers and the gneissic foliation. Pegmatite has collected at the boudin necks, commonly as elongate veins with an orientation oblique to the foliation and a consistent sense of asymmetry. At least two generations of pegmatite are present, and their mineralogy is greatly dependent on host lithology, suggesting that they represent, at least in part, locally derived partial melt.

An original intrusive contact appears to be preserved between the mafic and felsic lithologies within the hinge zone of the main synform, although the relative intrusive ages of the two lithologies are ambiguous.

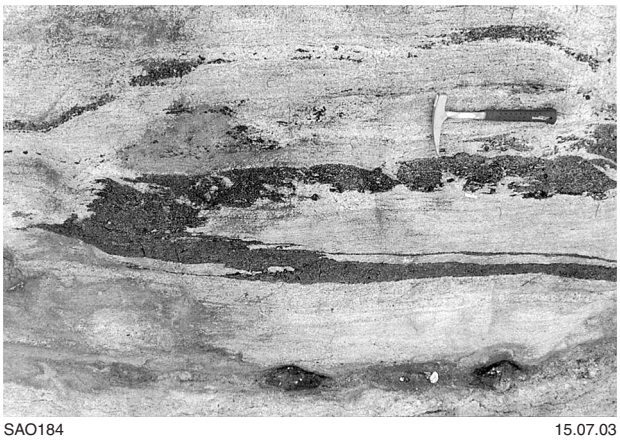

Figure 19. Tight to isoclinal F_1 folds in an amphibolite layer at Elephant Rock (Locality 8b). The foliation in the host granite gneiss is axial planar to the fold structures. North is to the right of the photograph

Locality 8c: Cape Hamelin

Walk around the coast south from Elephant Rock for about 700 m, and around Cape Hamelin to the east. The best structural features are preserved in the last 200 m of outcrop immediately before Deepdene Beach.

These outcrops comprise interleaved amphibolite and granite gneiss layers, typically 10–20 cm thick. These layers display a prominent foliation (which is variable due to later deformation, but generally trends about 040° and dips about 40°–70° to the west) and lineation (which plunges about 30° between 345° and 045°; Fig. 20). The amphibolite layers have been boudinaged during east-northeast – west-southwest extension, and then later shortened in the same direction, buckling the boudins and folding pegmatite veins that had formed at the boudin necks (Fig. 21). A 1.5 m-wide pegmatite dyke crosscuts all of these structures, and is relatively undeformed.

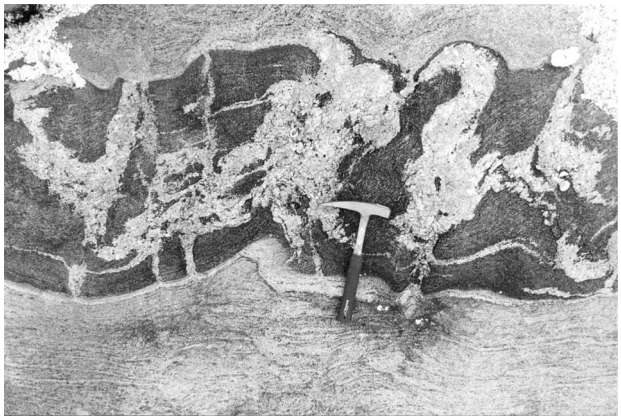

SAO186 15.07.03

Figure 21. Outcrop about 200 m east of Cape Hamelin (Locality 8c) illustrating D_3 buckling of an amphibolite layer that had been previously boudinaged during north–south D_1 extension. The folded pegmatite veins were originally situated in boudin necks. North is to left of the photograph

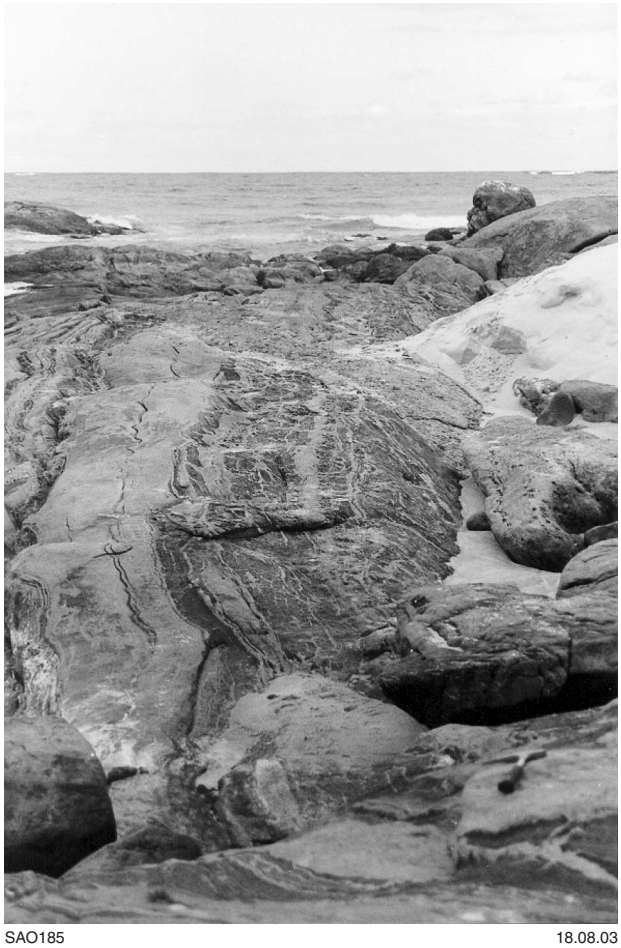

SAO185 18.08.03

Figure 20. Interlayered amphibolite and granite gneiss with steep westerly dips at Cape Hamelin (Locality 8c). Also visible is the D_3 buckling of the S_1 foliation and an undeformed pegmatite dyke that crosscuts all of these structures. Photograph was taken looking southwest

The easternmost outcrop, at the edge of Deepdene Beach, shows quite different structures to the other outcrops of this region, with asymmetric recumbent isoclinal folds displayed in an east–west vertical section, with the associated foliation having been folded. The hinges to these folds plunge about 30° towards 020°, which is broadly similar to other folds in the southern Leeuwin Complex, but axial planes are flat lying as opposed to steeply easterly dipping. The relationship of this outcrop to those exposed elsewhere in the southern Leeuwin Complex is unconstrained as yet, but is likely to be one of three possibilities. Firstly, these recumbent structures could be equivalent to the upright F_1/F_2 folds identified throughout the southern Leeuwin Complex, but folded by a later coaxial event, which rotated the axial planes, yet preserved the hinge lines. Secondly, the recumbent structures could be unrelated to F_1/F_2 and have developed within a later flat-lying high-strain zone that transposed the lower strain structures present elsewhere at this locality. Thirdly, the recumbent structures could have formed at some distal location by events that did not affect the southern Leeuwin Complex, and these rocks were brought together at some later stage. Whatever their origin, these flat-lying structures are critical to the evolution of the region since similar features are dominant throughout the central Leeuwin Complex (see **Localities 9**, **10**, **11**, **12a**, and **12b**).

Central Leeuwin Complex

Locality 9: Cape Freycinet

Return along Cosy Corner Road and turn left onto Caves Road. Follow Caves Road north, through the majestic karri trees of Boranup Forest for about 21 km to the Conto's Road turn-off (note that to stay on Caves Road you must turn right about 2 km north of the Cosy Corner Road junction). Turn left onto the bitumen Conto's Road. After 400 m, turn left and follow the sealed road west for another 1 km, where it changes to gravel by the turn-off to Conto's campground. Continue along the now gravel 2WD road for another 2.8 km, and turn right onto the gravel track signposted for Merchant Rock/Round Rock, and continue north for about 200 m to the Round Rock car park. Walk northwest for 200 m across the granite gneiss pavement, towards the large rounded outcrops near the coast.

This granite migmatite gneiss is garnet bearing and highly deformed. Most outcrop is dominated by a pervasive gneissic foliation that dips shallowly to the east, and a subhorizontal east-northeasterly trending lineation. However, one spot on the landward side of the big round boulder exposes a tapered lens of folds with subhorizontal hinges, wrapped around by the pervasive foliation (Fig. 22). The smooth outcrop face makes it difficult to measure fold orientations and it is unclear whether the hinges are parallel to the lineation developed in the enclosing LS-tectonites.

These structural relationships are quite different from those observed in the southern Leeuwin Complex, where outcrop-scale structures are dominated by steeply dipping foliations deformed by north-trending upright folds. Here it appears that a flat-lying pervasive foliation has largely transposed any earlier folds, and is associated with a lineation that is almost perpendicular to the lineation direction in the southern Leeuwin Complex.

SAO187 15.07.03

Figure 22. Isolated lens of folds within a garnet-bearing granite gneiss at Cape Freycinet (Locality 9). Outside of the region of folding, the pervasive gneissic foliation dips shallowly to the east. The hinges associated with this folding are probably parallel to the gently east-northeasterly plunging mineral lineation developed in the adjacent planar gneisses. Photograph taken looking west and the horizontal field of view is about 1.5 m

Locality 10: Redgate Beach

Drive back along Conto's Road and turn left onto Caves Road. Continue north along Caves Road for 7 km and turn left onto Redgate Road. Follow this bitumen road west and then south for about 3.5 km, where it ends in a large car park on the coast. Walk west from the northern end of the car park to the outcrops immediately below the plaque commemorating the wreck of the Georgette, and the rescue of the survivors by Grace Bussell and Sam Isaacs.

Rocks at Redgate Beach are similar to those at Cape Freycinet. Lithologically this outcrop comprises a garnet-bearing granite gneiss, which shows very little compositional variation and contains abundant leucosome veins. Outcrops are dominated by an intense foliation that dips shallowly to the northeast and a pervasive lineation that plunges gently down-dip. Feldspar augen indicate that the foliation is locally mylonitic and associated with high strain, but no consistent kinematic indicators have been identified. Asymmetric folds, with hinges parallel to the mineral-stretching lineation, are developed locally in-between the planar high-strain zones. Amphibolite layers form a minor component of the outcrop, and invariably lie within high-strain zones, suggesting that deformation was focused along the lithological contacts. These structures are crosscut by pegmatite veins that appear to form conjugate sets consistent with late east–west to southeast–northwest extension.

Two samples of this rock collected north of the monument have been dated by Nelson (1999) using SHRIMP U–Pb techniques, and contained dominant zircon populations with ages of 1091 ± 8 and 1091 ± 17 Ma. These ages are interpreted as the crystallization age of the igneous precursor in both cases, and are quite distinct from the younger protolith ages determined from rocks in the southern and northern Leeuwin Complex. Slightly older minor populations with imprecise ages of 1178 ± 40 and 1175 ± 98 Ma are interpreted as xenocrysts, whereas slightly younger populations of 1005 ± 46 and 1016 ± 10 Ma are thought to reflect an isotopic disturbance at this time. A single grain with an age of 531 ± 64 Ma is important, since it demonstrates that deformation and metamorphism of that age identified in the northern and southern Leeuwin Complex also affected these older protoliths.

Locality 11: Willyabrup Cliffs

Return to Caves Road, turn left and head north along Caves Road for about 26 km and turn left onto Willyabrup Road (Fig. 23), which is a gravel road. Follow this for 2.5 km — it doglegs right and then left along a fenceline — until arriving at a small parking area on the left, about 150 m after the left dogleg. Cross over to the south side of the fence, using the logs as steps, and follow the path along the fenceline westward down into a boggy patch (Biljedup Brook) and up again until meeting a north–south fence (about 200 m from the car park). At this point, cross back to the north side of the east–west fence, and continue west along the path. Another north–south trending fence crosses the path after 100 m; climb over this and follow the small track west for 20 m, where it meets the Cape-to-Cape

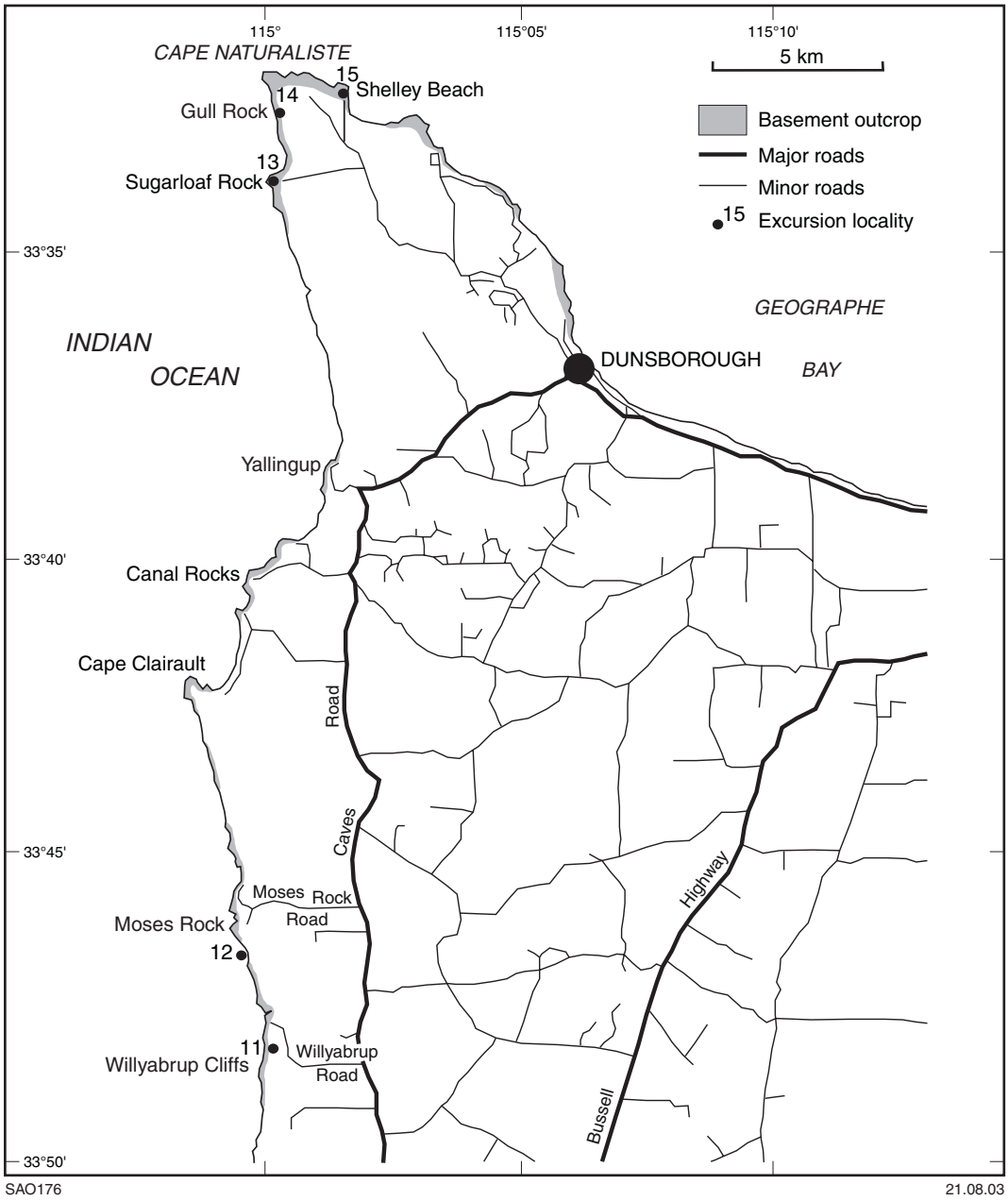

Figure 23. Map of the northern Leeuwin Complex showing Localities 11 to 15 and the extent of basement outcrop

walking track. At this point, turn right and follow the Cape-to-Cape track north, where it winds down into a wooded gully, and out to the coast. Turn left off the track at the base and walk back southward along the coastal rocks to the base of the cliffs.

Willyabrup Cliffs are dominated by flat-lying granite gneiss with a pervasive foliation that dips shallowly to the east. Gneisses that form the pavement at the base of the cliffs are grey in colour and locally garnet bearing, whereas those forming the tops of the cliffs weather to an orange colour and garnet is absent. Amphibolite layers several metres thick within the gneissic pile locally define isoclinal fold hinges that plunge gently to the northeast to east (Fig. 24), parallel to a widespread mineral-stretching lineation. These layers are commonly boudinaged, and pegmatite has migrated into the boudin necks during deformation. The amphibolite layers have a mineralogy that depends on the degree of strain. In layers of relatively low strain, the amphibolites are massive, and rich in deep-red garnet grains, which are commonly enclosed by a reaction rim of hornblende–plagioclase (Fig. 25). In high-strain layers the amphibolites are pervasively foliated and garnet is absent, but light-coloured ovoid patches are interpreted as former garnet grains completely replaced by hornblende and plagioclase during the deformation.

The presence of garnet in amphibolite is unusual for the Leeuwin Complex, which has been regarded as a low-pressure terrane because of a reported lack of garnet in

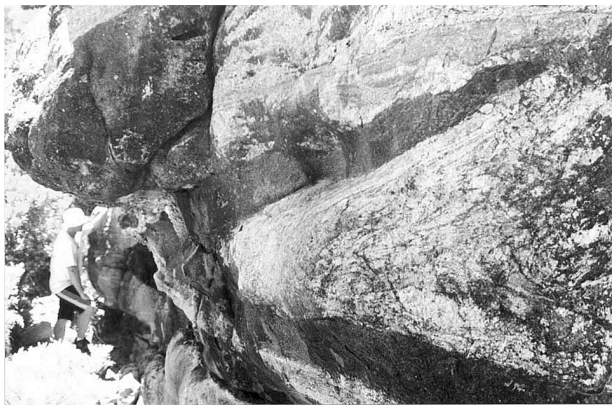

SAO188 15.07.03

Figure 24. Recumbent, tight to isoclinal fold in an amphibolite layer in granite gneiss at Willyabrup Cliffs (Locality 11). The fold deforms an earlier gneissic foliation in the granite gneiss. Photograph taken looking down-plunge (northeast)

SAO189 15.07.03

Figure 25. Plagioclase–hornblende reaction rims around garnet in an amphibolite horizon at Willyabrup Cliffs (Locality 11). These textures are consistent with decompression of the amphibolite from moderate- to low-pressure conditions. Diameter of the coin is 28 mm

mafic lithologies (Wilde and Murphy, 1990). Relationships at this locality imply that parts of the Leeuwin Complex experienced at least moderate pressures during metamorphism, and were exhumed during the deformation that produced flat-lying high-strain zones throughout the central Leeuwin Complex.

Locality 12a: Moses Rock

Return to the parking area, drive back along Willyabrup Road and turn left onto Caves Road. Continue north along Caves Road for about 5 km, and turn left onto Moses Rock Road. Follow this 2WD gravel road west for 3.3 km, where it ends at a T-junction. Turn left and follow the road south and then down a sandy slope to a car park behind the sand dunes, about 1.4 km from the T-junction. Walk northwest over the dunes towards Moses Rock, and stop after 200 m at the closest outcrop.

These rocks are granite gneisses with a shallow southeasterly dip and centimetre-scale leucosome veins that are predominantly parallel to, and to a large extent define, the pervasive gneissic foliation. They were described as pegmatite-veined Hamelin Granite by Myers (1994). Less-common pegmatite veins oblique to the foliation appear internally undeformed. The veins have narrow biotite selvages and there is no prominent lineation. A few hundred metres to the north, Myers (1994) mapped a layer of leucogabbro and anorthosite within the host granite gneiss. The dominant foliation has transposed any evidence of original intrusive contacts, and no folding is apparent, other than localized deflection of the foliation adjacent to the oblique melt veins.

Locality 12b: Honeycombs

Walk south along the beach, past the car park, for about 600 m to the nearest outcrops at the southern end of the beach.

Outcrops at the southern end of the beach are quite different from those at Locality 12a, and as is often the case in the Leeuwin Complex, the boundary between these rock types is concealed beneath a beach. These rocks comprise garnet-bearing granite gneiss, with a shallow easterly to southeasterly dip and prominent down-dip lineation. The lineation dominates within planar high-strain zones, which separate lower strain rocks that have been folded into asymmetric flat-lying structures with hinges parallel to the southeast-plunging lineation. The gneiss contains abundant centimetre-scale leucosome veins. Many of these are foliation parallel and have biotite-rich selvages along their margins, whereas a younger generation of oblique leucosome veins do not have selvages. Garnet is concentrated in the leucosome veins, indicating that much of it grew as a product of partial-melting reactions. Biotite- or hornblende-rich mafic layers, or both, within the granite gneiss are commonly the focus for pervasive deformation and the location of high-strain zones. No reliable kinematic indicators have been observed in the high-strain zones, and it is unclear whether these zones are regions of simple shear or rock packages where pure-shear strains have been greater in magnitude than elsewhere. Conjugate shear sets crosscut the pervasive fabrics, and their orientation and normal sense of movement are consistent with late northwest–southeast extension.

Unprocessed U–Pb SHRIMP zircon analyses from a sample of the garnet-bearing granite gneiss yield preliminary ages ranging from 750 to 500 Ma, with most of the younger ages coming from zircon rims, suggesting that a metamorphic event occurred at 550–500 Ma. An interpretation of the older cores and rims must await full processing of the data.

Northern Leeuwin Complex

Locality 13: Sugarloaf Rock

Drive back along Moses Rock Road, and turn left onto Caves Road. Continue north along Caves Road for about 13 km to a T-junction at Yallingup. Turn right at this junction, signposted as Caves Road to Dunsborough, and follow Caves Road for a further 8 km northeast to Dunsborough. Turn left into Cape Naturaliste Road, which is the first left turn at Dunsborough, and follow this winding road northwest for about 10 km and turn left onto Sugarloaf Road. Follow this bitumen road west for 2.8 km to reach the bottom car park. Walk 250 m west from the car park, up past the lookout, and down towards the distinctive 'hump' of Sugarloaf Rock. The outcrop of interest here is the 100 m-long peninsula that juts out to sea directly south of the islet of Sugarloaf Rock.

The rocks on the peninsula immediately south of Sugarloaf Rock comprise two main lithologies: pink-weathering, pegmatite-banded granite gneiss and grey, banded granodiorite gneiss (the Hamelin Granite and Cowaramup Gneiss of Myers, 1994). These rocks are folded into a D_2 antiform cored by the banded granodiorite gneiss and seamed with many granitic veins (Fig. 26). The contact between the two rock types is commonly parallel to the gneissic foliation, but there is local evidence that at least one phase of the granite gneiss crosscuts the compositional banding of the granodiorite gneiss. This relationship was used by Collins and Fitzsimons (2001) to suggest that the pegmatite-banded granite gneiss might have been emplaced after formation of the gneissic banding in the granodiorite gneiss, but it is unclear how much of the granodiorite gneiss foliation at the boundary has also been transposed by deformation.

Migmatitic segregations are common in the granodiorite gneiss, and also exist as nebulous massive veins crosscutting the pegmatite-banded granite gneiss. Foliation-parallel veins in the granite gneiss are difficult to see on many surfaces, but are clearly visible on weathered surfaces, where they are deformed into parasitic F_2 folds with east-dipping axial planes. Discrete amphibolite layers are parallel to the S_1 foliation in the pegmatite-banded granite gneiss and are commonly cut by pegmatitic veins. Metre-scale pegmatite veins crosscut the foliation of all rock types, but also appear to be folded in the core of the antiform. These observations suggest a close temporal relationship between partial-melt generation (thought to be at upper amphibolite – granulite facies) and D_2 deformation.

Four samples from this locality have been dated using SHRIMP U–Pb zircon techniques (Nelson, 2002; Collins, in press). All samples, from both the grey granodioritic core and the pink pegmatite-banded granite gneiss, yielded a spread of near-concordant zircon ages between 750 and 500 Ma. Two of the samples had well-defined zircon age populations at the older end of this spectrum, taken as evidence for igneous protolith crystallization at 730 ± 11 Ma (Nelson, 2002) and 746 ± 15 Ma (Collins, in press). Three of the samples had well-defined populations at the lower end of the age spectrum, taken as evidence

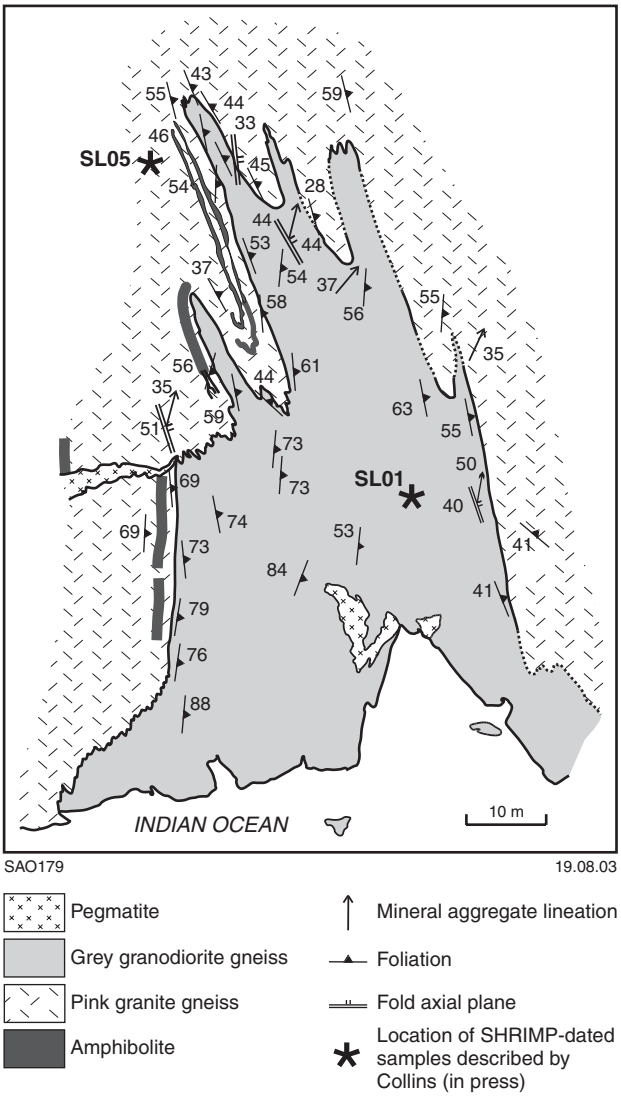

Figure 26. Detailed outcrop map of the D_2 Sugarloaf Antiform outcropping on the peninsula directly south of Sugarloaf Rock (Locality 13). Sampling sites for samples SL01 and SL05 dated by Collins (in press) are marked with asterisks

for significant isotopic disturbance at 542 ± 28 and 515 ± 19 Ma (Nelson, 2002) and at 522 ± 5 Ma (Collins, in press). Collins (in press) argued, using zircon growth structures and Th/U values, that this disturbance was caused by the metamorphic event responsible for the upper amphibolite- to granulite-facies mineral assemblages and partial-melting textures apparent in all lithologies of the area. This metamorphism resulted in solid-state recrystallization of magmatic zircon rims that had originally formed around the zircon cores at about 730 Ma or earlier.

Locality 14: Gull Rock

Drive back along Sugarloaf Road, and turn left onto Cape Naturaliste Road. Follow this road northwest for 2.2 km and turn left onto West Coast Road — a gravel road only

50 m before the car park for Cape Naturaliste lighthouse. Follow this road for 1.2 km westward up over the spine of Naturaliste Ridge and then northwest down towards the coast, and turn left onto another gravel track. Follow this track west and then south for 250 m to a car park. Walk along the path from the car park down to the beach. Gull Rock is the small island about 300 m south of the car park, and the outcrops of interest stretch northward along the foreshore for about 1 km from Gull Rock.

The outcrops immediately north of Gull Rock consist of banded granodiorite gneiss deformed into isoclinal folds with axial planes that dip about 40° to the northeast and hinges that plunge moderately to the north. Kilometre-scale mapping by Collins (in press; Figs 6 and 7) reveals that this part of the coast follows the axial trace of the regional-scale D_2 Naturaliste Antiform. About 200 m north of Gull Rock the outcrops become more massive, foliated rather than compositionally banded, and richer in K-feldspar. Structures in this granite gneiss are best preserved by discrete amphibolite layers that pick out a series of asymmetric S-folds plunging gently to moderately to the north, indicating that the regional antiform lies to the west. These folds become more symmetrical westward, towards the axial trace of the Naturaliste Antiform. North-plunging intersection lineations are commonly preserved at the contacts between the amphibolite and foliated granite gneiss, and are parallel to the D_2 fold hinges.

Locality 15: Shelley Beach, Bunker Bay

Drive back along West Coast Road and turn right onto Cape Naturaliste Road. Follow Cape Naturaliste Road southeast for 1.2 km and turn left onto Bunker Bay Road. Follow this road north for 1.2 km to the car park at the end, and then walk north along a track for 50 m to Shelley Beach, which lies in a small northeast-facing cove on the western side of Bunker Bay.

The promontory at the southeastern edge of the cove consists of K-feldspar-augen granite gneiss with a pervasive LS-tectonite fabric. The foliation dips moderately to the northwest, and mineral-aggregate lineations plunging down-dip on the foliation planes indicate a finite extension direction that is parallel to the regional plunge of the D_2 Naturaliste Antiform (Fig. 6). Kinematic indicators (sigma-type augen and C' shears) are locally preserved and indicate a top-down-plunge component of non-coaxial shear. Nebulous homogeneous granite veins cut the prominent lineations on the foliation planes, but contain a less well developed mineral lineation. Biotite–quartz patches throughout the rock may be original xenoliths.

Farther east around the point, the K-feldspar augen are less prominent and the rock is a homogeneous granite gneiss. To the south, on the western side of Bunker Bay, the gneiss is garnet bearing and contains prominent amphibolite units deformed into open folds. These folds plunge moderately to the northwest and have a down-plunge S-asymmetry attributed to the regional D_2 event.

The cliff at the northwest side of Shelley Beach exposes an unconformity between the granite gneiss of the Leeuwin Complex and the overlying Tamala Limestone (Fig. 27). The unconformity consists of a weathered saprolitic top to the Leeuwin Complex gneiss, overlain by a coarse boulder conglomerate capped by calcarenite of the Pleistocene–Holocene eolian Tamala Limestone. The conglomerate has a distinct planar upper surface, which was probably a wave-cut platform. The Tamala Limestone is not exposed east of this point in the Cape Naturaliste region, although it is widely exposed along the coast of Western Australia. The elevation of the unconformity surface of up to 10 m above sea level at Shelley Beach, as opposed to its near-sea-level exposure elsewhere, suggests significant neotectonic activity in the Cape Naturaliste region.

SAO190 15.07.03

Figure 27. Unconformity at Shelley Beach, Bunker Bay (Locality 15). There is an obvious wave-cut platform at about ten metres height above present sea level, with crystalline basement below, and the Pleistocene–Holocene Tamala Limestone above. Photograph taken looking west

The gneisses beneath the unconformity include a vertical 20 m-thick K-feldspar–biotite granite dyke, and a hornblende–two-pyroxene mafic granulite layer with abundant leucosome veins that outcrops at the base of the cliff. The leucosome veins cut across asymmetric folds in the mafic granulite, but are themselves partly deformed by the same folds, suggesting that partial melting occurred during deformation. This is supported by the concentration of other leucosomes in boudin necks produced by extension of the mafic granulite. Zircons from this mafic granulite unit have been dated using SHRIMP U–Pb techniques at 536 ± 21 Ma (Simons, 2001). Although this was interpreted by Simons (2001) as an intrusive age for the precursor mafic dyke, the high metamorphic grade of this rock and the widespread locally derived leucosomes suggest that these zircons could have grown during peak metamorphism and partial melting. Whatever the interpretation, these data provide further evidence that granulite-facies metamorphism in the Leeuwin Complex was Cambrian in age.

Drive back along Bunker Bay Road, turn left onto Naturaliste Road and continue southeast to the T-junction with Caves Road at Dunsborough. Turn left onto Caves Road, and continue east for 15 km to the Bussell Highway

turn-off. Turn right onto Bussell Highway, drive south for about 1 km and turn left onto the Busselton Bypass. Take the bypass east and continue along the Bussell Highway towards Bunbury and Perth.

Acknowledgements

We wish to thank the Department for Planning and Infrastructure for allowing access to the disused Roelands Granite Quarry, the Water Corporation for allowing access to the Harvey Weir Spillway, and the Department of Conservation and Land Management for approving field-trip movements through the Leeuwin–Naturaliste National Park.

References

ANDREWS, P. P., 1967, The geology of Cape Leeuwin, Western Australia: University of Western Australia, BSc (Hons) thesis (unpublished).

BAXTER, J. L., 1974, Murgoo, W.A.: Western Australia Geological Survey, 1:250 000 Geological Series Explanatory Notes, 23p.

BAXTER, J. L., and LIPPLE, S. L., 1985, Perenjori, W.A.: Western Australia Geological Survey, 1:250 000 Geological Series Explanatory Notes, 32p.

BEESON, J., HARRIS, L. B., and DELOR, C. P., 1995, Structure of the western Albany Mobile Belt (south-western Australia): evidence for overprinting by Neoproterozoic shear zones of the Darling Mobile Belt: Precambrian Research, v. 75, p. 47–63.

BESLIER, M.–O., LE BIHAN, T., FERAUD, G., and GIRARDEAU, J., 2001, Cretaceous ultra-slow spreading in the ocean–continent transition along the southwest Australian passive margin: constraints from 40Ar/39Ar dating: EUG XI abstract volume, Strasbourg, p. 718.

BLACK, L. P., SHERATON, J. W., TINGEY, R. J., and McCULLOCH, M. T., 1992, New U–Pb zircon ages from the Denman Glacier area, East Antarctica, and their significance for Gondwana reconstruction: Antarctic Science, v. 4, p. 447–460.

BLIGHT, D. F., and BARLEY, M. E., 1981, Estimated pressure and temperature conditions for some Western Australian Precambrian metamorphic terrains: Western Australia Geological Survey, Annual Report 1980, p. 67–72.

BLIGHT, D. F., COMPSTON, W., and WILDE, S. A., 1981, The Logue Brook Granite: age and significance of deformation zones along the Darling Scarp: Western Australia Geological Survey, Annual Report 1980, p. 72–80.

BORISSOVA, I., 2002, Naturaliste Plateau, a continental fragment: AUSGEO News, 67, p. 14–16.

BRETAN, P. G., 1986, Deformation processes within mylonite zones associated with some fundamental faults: University of London, Imperial College, PhD thesis (unpublished).

BRUGUIER, O., BOSCH, D., PIDGEON, R. T., BYRNE, D. R., and HARRIS, L. B., 1999, U–Pb chronology of the Northampton Complex, Western Australia — evidence for Grenvillian sedimentation, metamorphism and deformation and geodynamic implications: Contributions to Mineralogy and Petrology, v. 136, p. 258–272.

BYRNE, D. R., and HARRIS, L. B., 1993, Structural controls on the base-metal vein deposits of the Northampton Complex: Ore Geology Reviews, v. 8, p. 89–115.

CARROLL, D., 1940, Granitisation at Cape Leeuwin: Australian Journal of Science, v. 2, p. 167–170.

CARTER, J. D., and LIPPLE, S. L., 1982, Moora, W.A.: Western Australia Geological Survey, 1:250 000 Geological Series Explanatory Notes, 25p.

CAWOOD, P. A., and NEMCHIN, A. A., 2000, Provenance record of a rift basin: U/Pb ages of detrital zircons from the Perth Basin, Western Australia: Sedimentary Geology, v. 134, p. 209–234.

COBB, M. M., 2000, The age and origin of the Mullingarra Complex and its role in orogenic activity and the assembly of East Gondwana: Perth, Western Australia, Curtin University of Technology, BSc (Hons) thesis (unpublished).

COBB, M. M., CAWOOD, P. A., KINNY, P. D., and FITZSIMONS, I. C. W., 2001, SHRIMP U–Pb zircon ages from the Mullingarra Complex, Western Australia: Isotopic evidence for allochthonous blocks in the Pinjarra Orogen and implications for East Gondwana assembly: Geological Society of Australia, Abstracts, v. 64, p. 21–22.

COLLINS, A. S., in press, Structure and age of the northern Leeuwin Complex, Western Australia: constraints from field mapping and U–Pb isotopic analysis: Australian Journal of Earth Sciences, v. 50.

COLLINS, A. S., and FITZSIMONS, I. C. W., 2001, Structural, isotopic and geochemical constraints on the evolution of the Leeuwin Complex, SW Australia, *in* From basins to mountains: Rodinia at the turn of the century *edited by* K. N. SIRCOMBE and Z. X. LI: Geological Society of Australia, Abstracts, v. 65, p. 16–19.

COMPSTON, W., and ARRIENS, P. A., 1968, The Precambrian geochronology of Australia: Canadian Journal of Geological Sciences, v. 5, p. 561–583.

de LAETER, J. R., and LIBBY, W. G., 1993, Early Palaeozoic biotite Rb–Sr dates in the Yilgarn Craton near Harvey, Western Australia: Australian Journal of Earth Sciences, v. 40, p. 445–453.

DENTITH, M. C., BRUNER, I., LONG, A., MIDDLETON, M. F., and SCOTT, J., 1993, Structure of the eastern margin of the Perth Basin, Western Australia: Exploration Geophysics, v. 24, p. 455–462.

EMBLETON, B. J. J., and SCHMIDT, P. W., 1985, Age and significance of magnetizations in dolerite dykes from the Northampton Block, Western Australia: Australian Journal of Earth Sciences, v. 32, p. 279–286.

FITZSIMONS, I. C. W., 2000, Grenville-age basement provinces in East Antarctica: evidence for three separate collisional orogens: Geology, v. 28, p. 879–882.

FITZSIMONS, I. C. W., 2001, The Neoproterozoic evolution of Australia's western margin: Geological Society of Australia, Abstracts, v. 65, p. 39–42.

FITZSIMONS, I. C. W., 2002, Comparison of detrital zircon ages in the Pinjarra Orogen (WA) and Maud Province (Antarctica): evidence for collision of Western Australia with southern Africa at 1100 Ma: Geological Society of Australia, Abstracts, v. 67, p. 228.

FITZSIMONS, I. C. W., 2003, Proterozoic basement provinces of southern and south-western Australia, and their correlation with Antarctica, *in* Proterozoic East Gondwana: supercontinent assembly and breakup *edited by* M. YOSHIDA, B. F. WINDLEY and S. DASGUPTA: Geological Society of London, Special Publication 206, p. 93–130.

FITZSIMONS, I. C. W., in press, Mix and match: using zircon geochronology to correlate late Mesoproterozoic metamorphic belts in Antarctica and Western Australia: Geological Society of Australia, Abstracts.

FLETCHER, I. R., and LIBBY, W. G., 1993, Further isotopic evidence for the existence of two distinct terranes in the southern Pinjarra Orogen, Western Australia: Western Australia Geological Survey, Report 37, p. 81–83.

FLETCHER, I. R., WILDE, S. A., and ROSMAN, K. J, R., 1985, Sm–Nd model ages across the margins of the Archaean Yilgarn Block, Western Australia — III. The western margin: Australian Journal of Earth Sciences, v. 32, p. 73–82.

GIDDINGS, J. W., 1976, Precambrian palaeomagnetism in Australia I: basic dykes and volcanics from the Yilgarn Block: Tectonophysics, v. 30, p. 91–108.

GLIKSON, A. Y., and LAMBERT, I. B., 1973, Relations in time and space between major Precambrian shield units — an interpretation of Western Australian data: Earth and Planetary Science Letters, v. 20, p. 395–403.

GOLDSTEIN, S. L., O'NIONS, R. K., and HAMILTON, P. J., 1984, A Sm–Nd study of atmospheric dust and particulates from major river systems: Earth and Planetary Science Letters, v. 70, p. 221–236.

HARRIS, L. B., 1994a, Neoproterozoic sinistral displacement along the Darling Mobile Belt, Western Australia, during Gondwanaland assembly: Journal of the Geological Society of London, v. 151, p. 901–904.

HARRIS, L. B., 1994b, Structural and tectonic synthesis for the Perth Basin, Western Australia: Journal of Petroleum Geology, v. 17, p. 129–156.

HARRIS, L. B., 2003, Folding in high-grade rocks due to back-rotation between shear zones: Journal of Structural Geology, v. 25, p. 223–240.

HARRIS, L. B., and LI, Z. X., 1995, Palaeomagnetic dating and tectonic significance of dolerite intrusions in the Albany Mobile Belt, Western Australia: Earth and Planetary Science Letters, v. 131, p. 143–164.

HARRIS, L. B., HIGGINS, R. I., DENTITH, M. C., and MIDDLETON, M. F., 1994, Transtensional analogue modelling applied to the Perth Basin, Western Australia *in* The sedimentary basins of Western Australia *edited by* P. G. PURCELL and R. R. PURCELL: Petroleum Exploration Society of Australia, Western Australian Basins Symposium, Perth, W.A., 1994, Proceedings, p. 801–810.

HOCKING, R. M., van de GRAAFF, W. J. E., BLOCKLEY, J. G., and BUTCHER, B. P., 1982, Ajana, W.A.: Western Australia Geological Survey, 1:250 000 Geological Series Explanatory Notes, 27p.

HOPGOOD, A. M., and BOWES, D. R., 1995, Matching Gondwanaland fragments: the significance of granitoid veins and tectonic structures in the Cape Leeuwin – Cape Naturaliste terrane, SW Australia: Journal of Southeast Asian Earth Sciences, v. 11, p. 253–263.

KAY, J. G., 1958, The high-grade metamorphics of Cape Naturaliste, Western Australia: University of Western Australia, BSc (Hons) thesis (unpublished).

KRIEGSMAN, L. M., and HENSEN, B. J., 1998, Back reaction between restite and melt: implications for geothermobarometry and pressure–temperature paths: Geology, v. 26, p. 1111–1114.

KRIEGSMAN, L. M., MOLLER, A., and NELSON, D. R., 1999, P–T–t path and detrital zircon geochronology of the Northampton Block, Western Australia: a Mesoproterozoic, collisional induced foreland rift: Journal of Conference Abstracts, v. 4(1), p. 433.

LIBBY, W. G., and de LAETER, J. R., 1998, Biotite Rb–Sr age evidence for Early Palaeozoic tectonism along the cratonic margin in southwestern Australia: Australian Journal of Earth Sciences, v. 45, p. 623–632.

LIBBY, W. G., de LAETER, J. R., and ARMSTRONG, R. A., 1999, Proterozoic biotite Rb–Sr dates in the northwestern part of the Yilgarn Craton, Western Australia: Australian Journal of Earth Sciences, v. 46, p. 851–860.

LISTER, G. S., and PRICE, G. P., 1978, Fabric development in a quartz–feldspar mylonite: Tectonophysics, v. 49, p. 37–78.

LOGAN, B. W., and CHASE, L. R., 1961, The stratigraphy of the Moora Group: Royal Society of Western Australia, Journal, v. 44, p. 14–31.

LOW, G. H., 1975, Proterozoic rocks on or adjoining the Yilgarn Block, *in* The geology of Western Australia: Western Australia Geological Survey, Memoir 2, p. 71–81.

LOWRY, D. C., 1967, Busselton and Augusta, W.A.: Western Australia Geological Survey, 1:250 000 Geological Series Explanatory Notes, 22p.

McCULLOCH, M. T., 1987, Sm–Nd isotopic constraints on the evolution of Precambrian crust in the Australian continent, *in* Proterozoic lithospheric evolution *edited by* A. KROENER: American Geophysical Union, Geodynamics Series, v. 17, p. 115–130.

MURPHY, D. M. K., 1992, The geology of the Leeuwin Block, Western Australia: Perth, Western Australia, Curtin University of Technology, MSc thesis (unpublished), 164p.

MYERS, J. S., 1990a, Pinjarra Orogen, *in* Geology and mineral resources of Western Australia: Western Australia Geological Survey, Memoir 3, p. 265–274.

MYERS, J. S., 1990b, Anorthosite in the Leeuwin Complex of the Pinjarra Orogen, Western Australia: Australian Journal of Earth Sciences, v. 37, p. 241–245.

MYERS, J. S., 1993, Precambrian history of the West Australian Craton and adjacent orogens: Annual Reviews of Earth and Planetary Sciences, v. 21, p. 453–485.

MYERS, J. S., 1994, Late Proterozoic high-grade gneiss complex between Cape Leeuwin and Cape Naturaliste: Geological Society of Australia (W.A. Division), Excursion Guidebook 6, 26p.

MYERS, J. S., SHAW, R. D., and TYLER, I. M., 1996, Tectonic evolution of Proterozoic Australia: Tectonics, v. 15, p. 1431–1446.

NELSON, D. R., 1995, Field guide to the Leeuwin Complex: Third Australian Conference on Geochronology and Isotope Geoscience, Perth, W.A., 1995, Abstracts, 24p.

NELSON, D. R., 1996, Compilation of SHRIMP U–Pb zircon geochronology data, 1995: Western Australia Geological Survey, Record 1996/5, 168p.

NELSON, D. R., 1999, Compilation of SHRIMP U–Pb zircon geochronology data, 1998: Western Australia Geological Survey, Record 1999/2, 222p.

NELSON, D. R., 2002, Compilation of geochronological data, 2001: Western Australia Geological Survey, Record 2002/2, 282p.

NELSON, D. R., in prep., Compilation of geochronological data, 2002: Western Australia Geological Survey, Record 2003/2.

PEERS, R., 1971, The Proterozoic of the Geraldton–Northampton area: Western Australia Geological Survey, Annual Report 1970, p. 57–61.

PEERS, R., 1975, Northampton Block, *in* The geology of Western Australia: Western Australia Geological Survey, Memoir 2, p. 104–106.

PÉRON, F., and FREYCINET, L., 1807–1816, Voyage de découvertes aux Terre Australes, exécuté par ordre de sa majesté l'empereur et roi, sur les corvettes les Géographe, le Naturaliste, et la goélette Casuarina, pendant les années 1800, 1801, 1802, 1803 et 1804: Imprimerie Impériale, Paris.

PERRY, W. J., and DICKINS, J. M., 1960, Geology of the Badgeradda area, Western Australia: Australia Bureau of Mineral Resources, Report 46, 38p.

PISAREVSKY, S. A., WINGATE, M. T. D., POWELL, C. McA., JOHNSON, S., and EVANS, D. A. D., 2003, Models of Rodinia assembly and fragmentation, *in* Proterozoic East Gondwana: supercontinent assembly and breakup *edited by* M. YOSHIDA, B. F. WINDLEY, and S. DASGUPTA: Geological Society of London, Special Publication 206, p. 35–55.

PLAYFORD, P. E., HORWITZ, R. C., PEERS, R., and BAXTER, J. L., 1970, Geraldton, W.A.: Western Australia Geological Survey, 1:250 000 Geological Series Explanatory Notes, 39p.

PLAYFORD, P. E., COCKBAIN, A. E., and LOW, G. H., 1976, Geology of the Perth Basin, Western Australia: Western Australia Geological Survey, Bulletin 124, 311p.

POWELL, C. McA., PREISS, W. V., GATEHOUSE, C. G., KRAPEZ, B., and LI, Z. X., 1994, South Australian record of a Rodinian epi-continental basin and its mid-Neoproterozoic breakup (~700 Ma) to form the palaeo-Pacific Ocean: Tectonophysics, v. 237, p. 113–140.

POWELL, C. McA., and PISAREVSKY, S. A., 2002, Late Neoproterozoic assembly of East Gondwana: Geology, v. 30, p. 3–6.

PRIDER, R. T., 1948, The contact between the granitic rocks and the Cardup Series at Armadale: Royal Society of Western Australia, Journal, v. 27, p. 27–56.

SAINT-SMITH, E. C., 1912, A geological reconnaissance of a portion of the South-West Division of Western Australia: Western Australia Geological Survey, Bulletin 44, 80p.

SIMONS, S. L., 2001, Nature and origin of the mafic dykes within the late Proterozoic Leeuwin Complex, Western Australia: Perth, Western Australia, Curtin University of Technology, BSc (Hons) thesis (unpublished).

SIRCOMBE, K. N., and FREEMAN, M. J., 1999, Provenance of detrital zircons on the Western Australia coastline — implications for the geologic history of the Perth basin and denudation of the Yilgarn craton: Geology, v. 27, p. 879–882.

STOLZE, A., 2000, Structural and metamorphic investigation of part of the northern Leeuwin Complex: Perth, Western Australia, Curtin University of Technology, BSc (Hons) thesis (unpublished).

TORSVIK, T. H, CARTER, L. M., ASHWAL, L. D., BHUSHAN, S. K., PANDIT, M. K., and JAMTVEIT, B., 2001, Rodinia refined or obscured: palaeomagnetism of the Malani igneous suite (NW India): Precambrian Research, v. 108, p. 319–333.

WILDE, S. A., 1999, Evolution of the western margin of Australia during the Rodinian and Gondwanan supercontinent cycles: Gondwana Research, v. 2, p. 481–499.

WILDE, S. A., and LOW, G. H., 1980, Pinjarra, W.A.: Western Australia Geological Survey, 1:250 000 Geological Series Explanatory Notes, 31p.

WILDE, S. A., and MURPHY, D. M. K., 1990, The nature and origin of the Late Proterozoic high-grade gneisses of the Leeuwin Block, Western Australia: Precambrian Research, v. 47, p. 251–270.

WILDE, S. A., and NELSON, D. R., 2001, Geology of the western Yilgarn Craton and Leeuwin Complex, Western Australia — a field guide: Western Australia Geological Survey, Record 2001/15, 41p.

WILSON, A. F., COMPSTON, W., JEFFERY, P. M., and RILEY, G. H., 1960, Radioactive ages from the Precambrian rocks in Australia: Journal of the Geological Society of Australia, v. 6, p. 179–195.

WINGATE, M. T. D., and GIDDINGS, J. W., 2000, Age and palaeomagnetism of the Mundine Well dyke swarm, Western Australia: implications for an Australia–Laurentia connection at 755 Ma: Precambrian Research, v. 100, p. 335–357.

JANSSEN et al.

Structure and tectonics of the Leeuwin Complex and Darling Fault Zone, southern Pinjarra Orogen, Western Australia — a field guide

RECORD 2003/15

Further details of geological publications and maps produced by the Geological Survey of Western Australia can be obtained by contacting:

Information Centre
Department of Industry and Resources
100 Plain Street
East Perth WA 6004
Phone: (08) 9222 3459 Fax: (08) 9222 3444
www.doir.wa.gov.au

View publication stats